horticulturae

MDPI

Article

Integrated Transcriptomic and Metabolomic Analysis Reveals the Characteristics of Flavonoid Biosynthesis in *Spatholobus suberectus*

Daocheng Ma [1,†], Dandan Yang [1,†], Jun Liu [2], Meimei Luo [1], Xiuhua Zhang [2], Mei Yang [1] and Yuanyuan Xu [1,*]

[1] Guangxi Key Laboratory of Forest Ecology and Conservation, Key Laboratory of National Forestry and Grassland Administration on Cultivation of Fast-Growing Timber in Central South China, College of Forestry, Guangxi University, Nanning 530004, China; madaochengmail@163.com (D.M.); dandan_n@yeah.net (D.Y.); 2309302014@st.gxu.edu.cn (M.L.); lyangmei@gxu.edu.cn (M.Y.)

[2] Guangxi State-Owned Qipo Forest Farm, Nanning 530225, China; liujunmail2026@163.com (J.L.); xiuhua1005421@163.com (X.Z.)

* Correspondence: yuanyuanxu@gxu.edu.cn

† These authors contributed equally to this work.

Abstract

Spatholobus suberectus is a traditional edible, ornamental, and medicinal vine with an abundant flavonoid content in its dried stems. An integrated metabolomic and transcriptomic analysis was conducted on its vegetative organs to identify flavonoid biosynthesis pathways. The results showed that: (1) a total of 268 flavonoids could be identified among all the vegetative organs, and stems accumulated most of them; (2) a total of 449,569,220 clean reads were retained from all the vegetative organs (many genes related to key enzymes of flavonoid biosynthesis and transcription factors were found in all the compared groups between different organs; among them, 77 genes showed high correlations with key flavonoids in different pathways); and (3) *PAL* (encoding phenylalanine ammonia-lyase), *4CL* (encoding 4-coumarate: CoA ligase), *C4H* (encoding cinnamate-4-hydroxylase), *CHS* (encoding chalcone synthase), *DFR* (encoding dihydroflavonol 4-reductase) and others showed positive correlations with L-phenylalanine and various flavonoids, while *FLS* (encoding flavonol synthase) showed negative correlations with many flavonols and flavonoids, as revealed through integrated analysis. This study reveals the flavonoid biosynthesis characteristics in *S. suberectus* and provides new insights into the utilization of its biological resources.

Keywords: flavonoid biosynthesis; different vegetative organs; transcriptomics; metabolomics; *Spatholobus suberectus*

Check for updates

Academic Editor: Jiri Gruz

Received: 9 April 2026
Revised: 20 May 2026
Accepted: 20 May 2026
Published: 23 May 2026

Copyright: © 2026 by the authors. Licensee MDPI, Basel, Switzerland. This article is an open access article distributed under the terms and conditions of the Creative Commons Attribution (CC BY) license.

1. Introduction

Spatholobus suberectus (family Fabaceae) is a kind of large woody ornamental and medicinal vine that inhabits the understory of southern China (Guangxi, Yunnan, Guangdong, Fujian, and other provinces) and many South Asian countries, with high antiviral and anti-cancer activities, such as scavenging free radicals and anti-inflammatory effects [1,2]. Its dried stem was widely used as an ethnomedicine (named "Jixueteng" in Chinese), as it contains abundant flavonoids, sterols, triterpenes, and organic acids and has a high medicinal value. Flavonoids are dominant, and the stem can be sliced into pieces and added to soups to enhance their taste and smell [3]. In the early 2000s, some pterocarpans,

flavanones, isoflavanes and isoflavones (like (6aR,11aR)-maackiain/medicarpin, sativan, pseudobaptigenin, genistein, etc.) were identified in its stems, indicating that it has high antioxidant and blood-activating activities [4]; some other flavonoids (such as genistein, isoliquiritigenin, medicarpin, naringenin, etc.) from *S. suberectus* were also isolated and identified [5]. At present, the stems of wild *S. suberectus* are harvested in large quantities for medicinal use, causing a serious shortage of resources. In order to alleviate the resource shortage and due to its shade tolerance, *S. suberectus* has been widely artificially planted in the Guangxi Zhuang Autonomous Region in recent years (especially under pine forests), establishing the "forest-medicine" multilayer cultivation mode to enhance the integrity of forest ecosystems [6,7]. After about 6 years of artificial cultivation, its medicinal quality was similar to that of plants grown in wild environments. Many leaves and roots (also abundant in flavonoids and other components) were left after stem harvesting. How to efficiently use the roots and leaves of *S. suberectus* should be further investigated. In summary, flavonoids are the dominant chemical components in *S. suberectus*, with high medicinal value and application prospects, and it is important to explore the contents of flavonoids and other chemical components in all the vegetative organs; the biosynthesis process could improve the bioresource utilization of *S. suberectus*.

Flavonoids are the dominant secondary metabolites and the main chemical components of many medicinal plants. Generally speaking, flavonoids can be found throughout all plants and seedlings, although their accumulation characteristics may differ significantly [8]. For example, some woody/herbal vines and medicinal plants accumulate abundant flavonoids in their stems. As for *Vitis davidii*, proanthocyanidins (PAs) can be found in its skins, seeds, and stems [9]. In addition, the categories and content of flavonoids are different in various organs and species. For example, flavonoids are abundant in both the stems and leaves of *Vitis vinifera*. Quercetin (a kind of flavonol) and its derivatives are the main flavonoids in leaves, while catechin and some other flavonoids are dominant in stems [10], and the flavonoid content in roots increases under some stress conditions [11]. But in some subspecies of *Vitis vinifera* ('*Djebba*', '*Ouchtata*', and so on), flavonoids accumulate more in roots than stems [12]. *Pueraria thomsonii* and *P. lobate* have more fiber, isoflavones, flavonoids and (crude) protein than *P. thomsonii*, causing differences in their medicinal and edible values [13]. Flavonoids are abundant in the leaves and flowers of *Semiliquidambar cathayensis* rather than the stems and roots, but some organic acids (ursolic and oleanolic acids, etc.) mainly accumulate in the roots [14]. In summary, flavonoids and many other chemical components have different accumulation characteristics in various plants. It is significant for researchers to know the main kinds and contents of active compounds in different organs in order to choose suitable medicinal parts and improve the utilization value of the other parts of plants.

Flavonoid biosynthesis is also influenced by some key genes, including genes involved in flavonoid synthesis, genes encoding flavone and flavonol-related synthase, and genes encoding transcription factors that collaboratively regulate key enzyme activities [8]. For example, the expression of the *VvFLS1* gene was related to flavonol content among buds, leaves, and other organs of *V. vinifera* [15]. *FmPAL1*, *FmPAL2*, and *FmPAL3* of *Fallopia multiflora* were highly expressed in stems and leaves rather than roots. All of them were related to phenylalanine and flavonoid biosynthesis [16]. The expression levels of *PAL1–7*, *CHS2*, *FNSII*, and some other genes in the rhizomes of *Houttuynia cordata* were related to apigenin content [17]. In a cultivar of *Vitis vinifera* ('Cabernet Sauvignon'), the up-regulation of *VvDFR*, *VvUFGT*, and *VvOMT* would increase the anthocyanin content [18]. In *Pueraria montana* var. *lobata*, *UGT*, *bHLH*, *C4H*, and other genes directly regulated daidzein, genistein and other isoflavonoids contents in root tubers [19]. The expression levels of *F3H*, *F3′5′H*, *CHS*, and many other genes were related to the contents of kaempferol, luteolin, and

other flavonoids in purple passion (*Passiflora edulis*) fruits [20]. Many DEGs (Differential Expressed Genes) were also enriched in the flavonoid biosynthesis pathway (*CHI*, *FLS*, *3GT*, *DFR*, *CHS*, etc.) between young and mature leaves of *Ampelopsis grossedentata*, possibly related to flavonoid biosynthesis [21]. Similar results were also observed in *Uncaria rhynchophylla* (*F3H*, [22]) and *Gynostemma pentaphyllum* (*DFR*, *GGPPS*, and others, [23]). Similar phenomena were also observed in many other vine plants. E-resveratrol, E-piceatannol, and some other phenylpropanoid/flavonoids in grapevine could be found in canes, buds, and other tissues, while *VviMYB14* and other key genes encoding transcription factors were significant during flavonoid biosynthesis [24]. In addition, flavonoid biosynthesis was also related to some transcription factors (like MYB, bHLH, WRKY, AP2/ERF, etc.) and their encoding genes, which had different regulatory effects on key enzyme genes [25–27]. So, genes encoding transcription factors could be also collaboratively influenced by key enzyme activities, which played important roles in the process of plant flavonoid biosynthesis.

In recent years, some basic research has emerged on flavonoid biosynthesis in *Spatholobus suberectus*. For example, some genes and transcription factors in the IFS and MYB families were shown to possibly regulate flavonoid biosynthesis in its vine stems [28–30]. But the quantitative analysis and partial transcriptome sequencing of flavonoids only focused on the main medicinal parts, the stems, in these studies. The in-depth relationships between the transcriptome/metabolome and resource utilization were lacking, and the mechanism of gene regulation of the main medicinal components was still unclear. Finding out the distribution and accumulation characteristics of the main chemical components in each vegetative organ and understanding the internal mechanism of flavonoid biosynthesis are important for bioresource utilization. Based on this, this study used the vegetative organs (root, stem, and leaf) of *S. suberectus* under a *Pinus elliottii* forest in Guangxi State-Owned Qipo Forest Farm as the research materials, analyzed flavonoid accumulation characteristics in the roots, stems, and leaves of 6-year-old plants, and conducted transcriptome and metabolome analyses between them. We hypothesized that: (1) Except for flavonoids, there would be various other chemical components among all the vegetative organs of *S. suberectus* that could be further used. Some specific flavonoids in the stem might be highly correlated with its color and pharmacodynamic quality; and (2) DAMs (Differential Accumulated Metabolites) and DEGs enriched in the biosynthesis pathways of phenylpropanoid, flavonoids, and isoflavonoids could be found in all the compared groups, showing different positive and negative correlations. Some genes encoding key transcription factors also played important roles in (iso) flavonoid biosynthesis. The study's objectives were: (1) to identify the differences in metabolites in different vegetative organs of *S. suberectus* and evaluate the value of development and utilization of other organs except the vine stem; and (2) to clarify the biosynthesis mechanism of flavonoids by integrated transcriptomic and metabolomic analysis, screening key unigenes and potential TFs (transcription factors) related to flavonoid synthesis. This study reveals the accumulation traits of different medicinal ingredients in *S. suberectus* as well as the directed cultivation and high-quality utilization of this species, and it can also guide the efficient utilization of other organs except vine stems.

2. Materials and Methods

2.1. Plant Materials

Roots, stems, and leaves of 6-year-old *S. suberectus* were collected under a 50 year-old *Pinus elliottii* forest in Guangxi State-Owned Qipo Forest Farm (Nanning), China (108°12′25″ E, 22°42′18″ N), with a subtropical monsoon climate (21.6 °C mean annual temperature, 1350 mm mean annual precipitation). The test site was a hilly area with an altitude of 90–280 m and slopes of 10~40°. The height of the trees was 40~50 m, the

average thickness of the acidic red soil layer was about 80 cm, and the planting density was 600 trees per hectare. In 2017, 0.5-month-old *S. suberectus* cutting seedlings were planted under the *P. elliottii* forest. On 14 July 2023, all the samples were collected for transcriptomic and metabolomic analysis. Three biological replicates were collected for each organ (three seedlings were mixed as one replicate), and samples were frozen in liquid N_2 and stored at −80 °C.

2.2. Metabolome Analysis

(1) Metabolite extraction and HPLC/MS conditions: The root, stem, and leaf samples after freeze-drying were powdered by a grinder (MM 400 from Retsch, Hamburg, Germany). Then, 1200 μL of 70% methanolic (aq) solution was added into 50 mg of each sample for standard extraction (vortexed 6 times, every 0.5 h for 30 s each). The supernatant was aspirated after 12,000 rpm for 3 min and then stored in sampling vials (through 0.22 μm membrane) for the next step of analysis. Details of HPLC and MS conditions are provided in the Word document of the Supplementary Materials (Supplementary Tables S1 and S2). Quality control (QC) samples were prepared by pooling equal volumes of all sample extracts. QC samples were injected every 10 analytical samples to monitor instrument stability. Metabolite features with a relative standard deviation (RSD) > 30% in QC samples were excluded from further analysis.

(2) Differential metabolites analysis: Principal component analysis (PCA) was used for statistical analysis between different organs. DAMs had to satisfy the conditions of VIP > 1, p-value < 0.05 and $|\log_{2f}\text{old change}| \geq 1$, and these were then mapped into different biochemical KEGG pathways via http://www.genome.jp/kegg/, and enrichment analysis was conducted. Finally, heatmaps were made via the gplot R package 2.0.

2.3. Transcriptome Analysis

(1) RNA extraction, library construction, and Seq-analysis: Total RNA was extracted from three independent replicates of *S. suberectus* root, stem, and leaf. After extraction, RNA purity was checked by a Nano Photometer® spectrophotometer (IMPLEN, Westlake Village, CA, USA). A NEBNext® Ultra™ RNA Library Prep Kit for Illumina® (NEB, Ipswich, MA, USA) was used for preparing sequencing libraries. mRNA was purified from total RNA by poly-T oligo-attached magnetic beads, and fragmentation was carried out using divalent cations under an elevated temperature in NEBNext First Strand Synthesis Reaction Buffer (5×). Subsequently, the first and second strands of cDNAs were synthesized by random hexamer primer and MMuLV Reverse Transcriptase (RNase H-) and DNA Polymerase I (RNase H). The NEBNext Adaptor was prepared for hybridization after adenylation of the 3′ ends of DNA fragments. Finally, the library fragments were purified, and the cDNA was amplified by PCR.

(2) Quality control and transcriptome assembly: Clean reads were isolated from all the raw data (by removing low-quality reads with quality values ≤ 10). Q20, Q30, and the GC content of the clean reads were calculated. Transcriptome assembly was accomplished based on the left.fq and right.fq using Trinity (version 2.15.1). The assembled transcripts were hierarchically clustered into unigenes using shared reads and expression by Corset.

(3) Bioinformatics analysis: De novo unigenes were annotated through different pathway databases (based on BLAST (Basic Local Alignment Search Tool, 2.12.0) to search with an E-value threshold of 1×10^{-5}). The DESeq R package (1.18.0) was used to identify DEGs between two different groups. The resulting p-values were adjusted using the Benjamini–Hochberg approach for controlling the false discovery rate. Genes with an adjusted p-value < 0.05 and $\log_2$(fold change) > 1 found by DESeq were considered differentially expressed. In addition, the KEGG (Kyoto Encyclopedia of Genes and Genomes)

database was used to further analyze DEGs, and the expression level of these genes was analyzed by the KOBAS software (KEGG Orthology-Based Annotation System, version 3.0) and KEGG website (http://www.genome.jp/kegg/). Finally, the PlantTFDB database (http://planttfdb.gao-lab.org/) was used to analyze transcription factors, and heatmaps were drawn by gplot R package.

2.4. qRT-PCR Analysis

The expression level of ten unigenes related to key enzymes and transcription factors of (iso) flavonoid biosynthesis was analyzed by qRT-PCR. Total RNA was extracted via the Trizol method. Then, a KangWei Century kit (from Taizhou, Jiangsu, China) and specific primers were used and designed to perform reverse transcription and cDNA/primer synthesis. The system of qRT-PCR consisted of template cDNA (1 μL), forward/reverse primers (0.7 μM for each), 2× SYBR Green PCR Master Mix (5 μL), QN ROX Reference Dye (0.05 μL), and RNase-free water (2.55 μL), totaling 10 μL. The 846-x-070-301 real-time PCR System (provided by Biometra TONE, Shanghai, China) was used for qRT-PCR analysis (with an annealing temperature of 60 °C). Each unigene was tested with 3 biological replicates. The $2^{-\Delta\Delta Ct}$ method was used for quantitative data analysis.

3. Results

3.1. Metabolome Analysis Results

(1) General information for identification of all metabolite types

The results of LC-MS/MS among all the vegetative organs of *S. suberectus* showed that there were 2470 metabolites in the POS mode and 1570 metabolites in the NEG mode (totaling 4040, Supplementary Table S3). Among all metabolites, amino acids (and derivatives), benzene and substituted derivatives, organic acids, flavonoids, alkaloids and terpenoids were the dominant components among all the vegetative organs. Amino acids and derivatives (1010, 25.00%) were mainly distributed in leaves (leaf>stem>root), as well as phenolic acids, lipids, and heterocyclic compounds; organic acids (556, 13.76%), benzene and substituted derivatives (486, 12.03%) and flavonoids (268, 6.63%) were mainly distributed in stems (stem>leaf>root), while alkaloids (169, 4.18%) and terpenoids (114, 2.82%) were mainly distributed in roots (root>leaf>stem) (Figure 1A and Supplementary Figure S1A,B). Flavones, flavonols, flavanols, and dihydroisoflavones were dominant in roots; isoflavones, and biflavones were dominant in stems; anthocyanidins, chalcones and flavanones were the major categories in *S. suberectus* leaves (Figure 1C). In addition, significant differences in metabolite clustering among different organs could be found through PCA analysis, and all replicates of the same organs were clustered together under both positive and negative modes, indicating that metabolite categories varied greatly among different organs and that the repeatability of this experiment was good (Supplementary Figure S1C,D).

(2) Categories and relative quantitative content of different flavonoids

Due to the accumulation characteristics of *Spatholobus suberectus*, we analyzed the relative quantitative content of flavonoids in its roots (R), stems (S) and leaves (L) (Figures 1B,C and 2). The results indicated that there were a total of 268 compounds among all the organs, including 99 flavones, 40 flavonols, 31 isoflavones, 24 anthocyanidins, 17 chalcones, 13 flavanones, 12 flavanols, 4 flavanonols, 2 biflavones, 1 dihydroisoflavone and 25 other flavonoids (Supplementary Table S4). Some major species (flavanols, flavonols, flavones) mainly accumulated in stem. Flavones accounted for 36.94% of all flavonoids, and the top five in stems were robinetinidol-(4alpha->8)-catechin-(6->4alpha)-robinetinidol, L-epicatechin, neoschaftoside, gossypetin 8-glucuronide 3-sulfate and vitexin 2″-O-rhamnoside. Flavonols (40, 14.93%, the top five in stem were kaempferol-3-O-(2″-p-coumaroyl) galactoside, rhamnetin, quercetin, isorhamnetin 3-galactoside and kaempferol

3-O-beta-D-galactopyranosyl-7-O-alpha-L-rhamnopyranoside), isoflavones (31, 11.57%, the top five in stem were ononin, genistin, formononetin, 7-hydroxy-3-(2-methoxyphenyl)-4H-chromen-4-one and 5-methyl-7-methoxyisoflavone), anthocyanidins (24, 8.96%, the top five in stem were pelargonidin 3-O-(6-caffeoyl-beta-D-glucoside), pelargonidin 3-O-beta-D-sambubioside, delphinidin 3-O-(6″-O-malonyl)-beta-D-glucoside-3′-O-beta-D-glucoside, peonidin pentose and peonidin 3-(6″-acetylglucoside), and chalcones (17, 6.34%, the top five in stem were pinostrobin chalcone, 4′-methoxychalcone, naringenin-4′-o-beta-d-glucuronide, isoliquiritigenin, and cardamonin) were also dominant. Among the stems, ononin, genistin, formononetin, kaempferol, quercetin and L-epicatechin had strong antioxidant and anti-bacterial activities in various medicinal and aromatic plants, while pelargonidin was the main kind of anthocyanidin, showing the deep purple–red color of *S. suberectus* stems. Some of them also accumulated in roots and leaves (Supplementary Table S4). In summary, the color and pharmacodynamic quality of *S. suberectus* stems were closely related to some specific flavonoids (flavonols) and anthocyanins. However, its leaves and roots were rich in amino acids, terpenoids and alkaloids, which may have high edible or medicinal value and deserve further investigation.

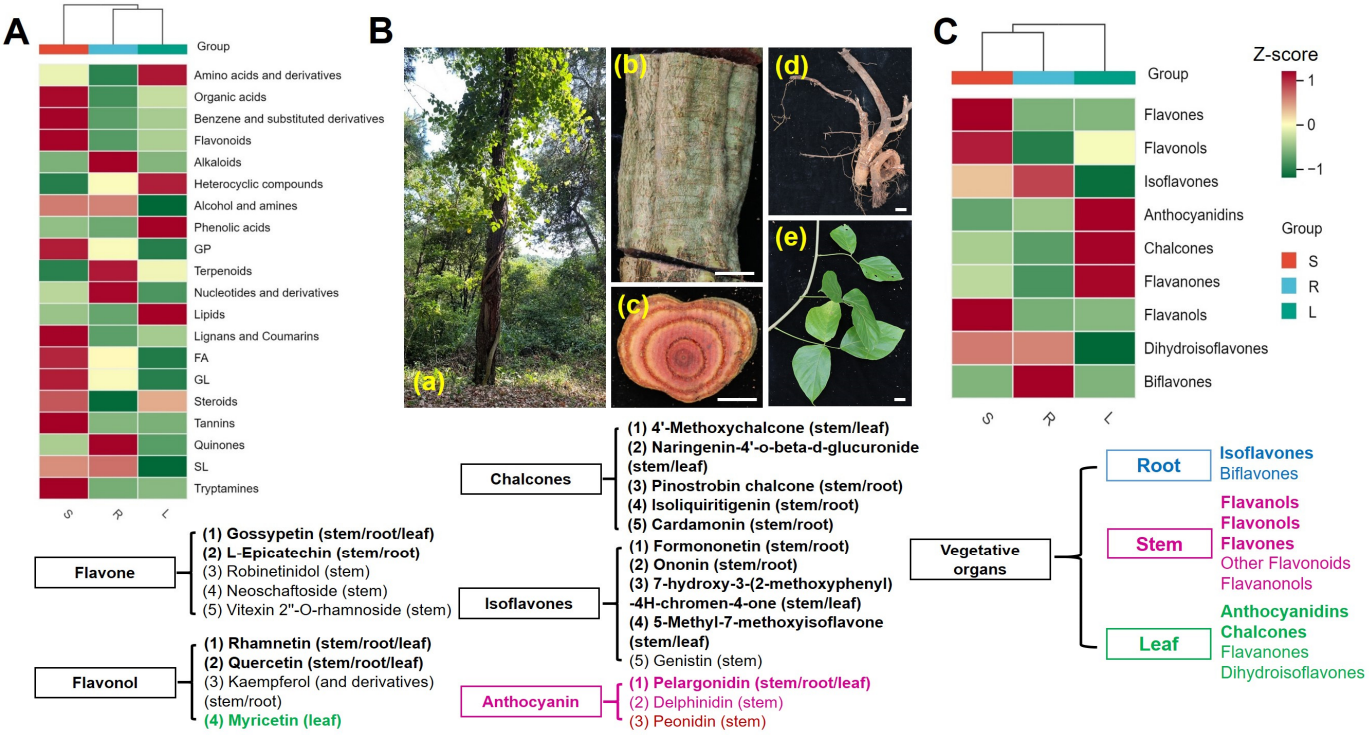


Figure 1. The main metabolites in all the vegetative organs of *S. suberectus* ((**A**): heatmap of different kinds of metabolites in the vegetative organs of *S. suberectus*; (**B**): understory environment and morphological characteristics of *S. suberectus*; (**a**): understory site for *S. suberectus* cultivation; (**b**,**c**): stem of *S. suberectus*; (**d**): roots of *S. suberectus*; (**e**): leaves of *S. suberectus*; (**C**): heatmap of flavonoid subclasses in the vegetative organs of *S. suberectus*; heatmaps in (**A**,**C**) show the gene expression abundance among various organs, and the color bar from −1 to 1 represents the Z-score of DAM levels after standardization, with the same in Figure 2; the length of the white bars in (**B**) represents 2 cm).

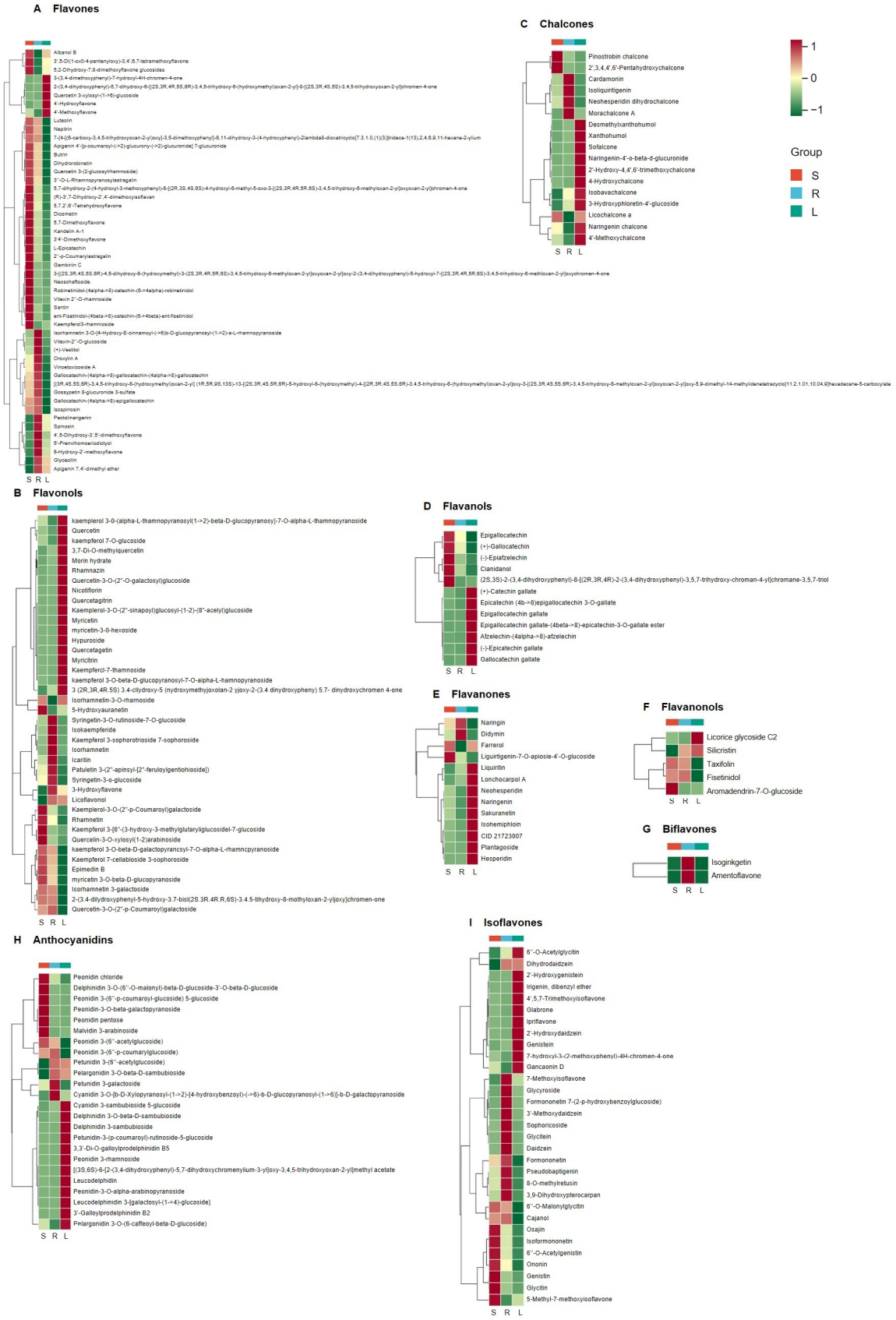


Figure 2. Different kinds of flavonoids in different organs of *S. suberectus* ((**A**): flavones (top 50 compounds in all the organs); (**B**): flavonols; (**C**): chalcones; (**D**): flavanols: (**E**): flavanones; (**F**): flavanonols; (**G**): biflavones: (**H**): anthocyanidins; (**I**): isoflavones).

(3) Differences in metabolite accumulation among all the vegetative organs and enrichment analysis

DAMs were analyzed between different vegetative organs (roots, stems and leaves) by VIP > 1 and $\log_2$ fold change ($|\log_2 FC| \geq 1$) conditions, and the results can be seen in Figure 3. It could be seen that stems and roots were divided into the same cluster, while leaves were grouped in another one in the results of the hierarchical clustering analysis (Figure 3A), indicating that there were more differences between leaves and the other organs than between roots and stems. As for the expression trends of the identified DAMs, subclasses 1, 2 and 3 showed different trends, while roots, stems, and leaves had the highest metabolite abundances, respectively (Figure 3B). A total of 868 DAMs (totaling 2589, 2556, and 1993 DAMs in L vs. R, L vs. S, and R vs. S groups) existed among all the three comparison groups (L vs. R, L vs. S, and R vs. S) (Figure 3C). Among these three groups, there were 1596, 1686, and 1166 up-regulated DAMs and 993, 870 and 827 down-regulated DAMs (Figure 3D).

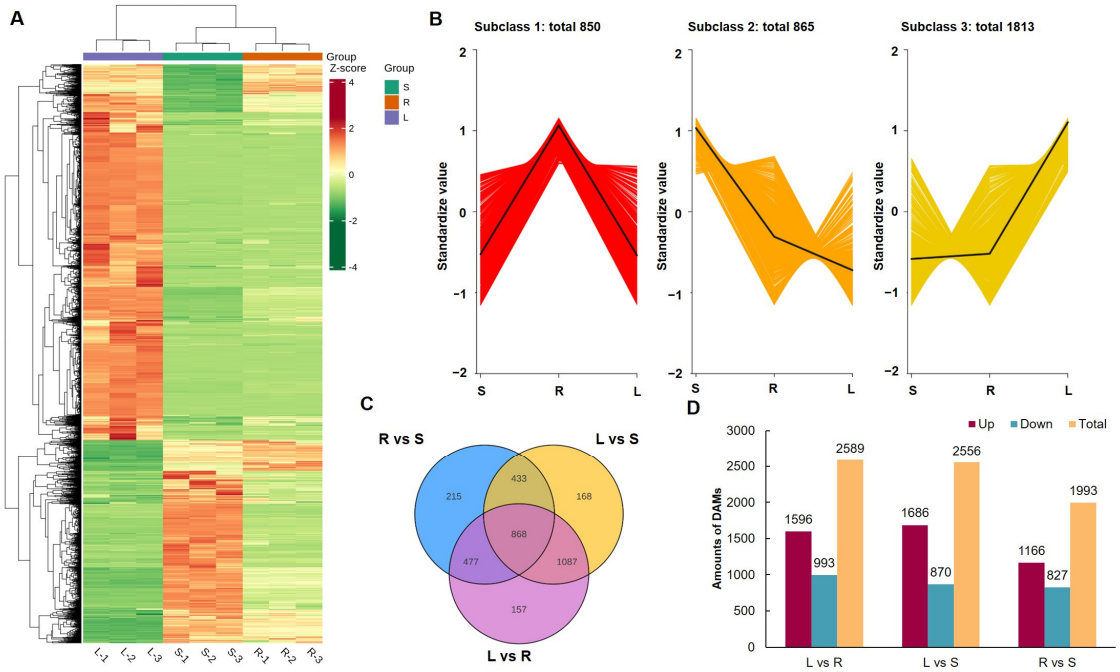


Figure 3. Amounts and cluster analysis of DAMs among different organs of *S. suberectus* ((**A**) hierarchical clustering analysis of the identified DAMs across different organs. The horizontal axis represents the sample clusters, and colors from green to red indicate metabolite accumulation levels from low to high; (**B**) the expression trends of the identified DAMs; (**C**) Venn diagram of the shared and unique DAMs among all the vegetative organs; (**D**) numbers of up-regulated and down-regulated DAMs in comparisons between different organs).

(4) Identification analysis of flavonoid-related metabolites among all the vegetative organs of *S. suberectus*

Among all the compared groups, DAMs were significantly enriched in the following five pathways: ko00940 (phenylpropanoid biosynthesis), ko00941 (flavonoid biosynthesis), ko00942 (anthocyanin biosynthesis), ko00943 (isoflavonoid biosynthesis) and ko00944 (flavone and flavonol biosynthesis). We focused on these pathways and the related metabolites (Figure 4A–D). Among all the organs, there were a total of 230 compounds related to flavonoids, including 80 flavones, 36 flavonols, 27 isoflavones, 20 anthocyanidins, 15 chalcones, 12 flavanols, 11 flavanones, 2 flavanonols, 2 biflavones, 1 dihydroisoflavone, and 24 other flavonoids (Figure 4E and Supplementary Table S5). Flavones accounted for 34.78% of all flavonoids, indicating that they were the major category among all flavonoids.

In addition, flavonols (36, 15.65%), isoflavones (27, 11.74%), anthocyanidins (20, 8.70%) and chalcones (15, 6.52%) were also dominant.

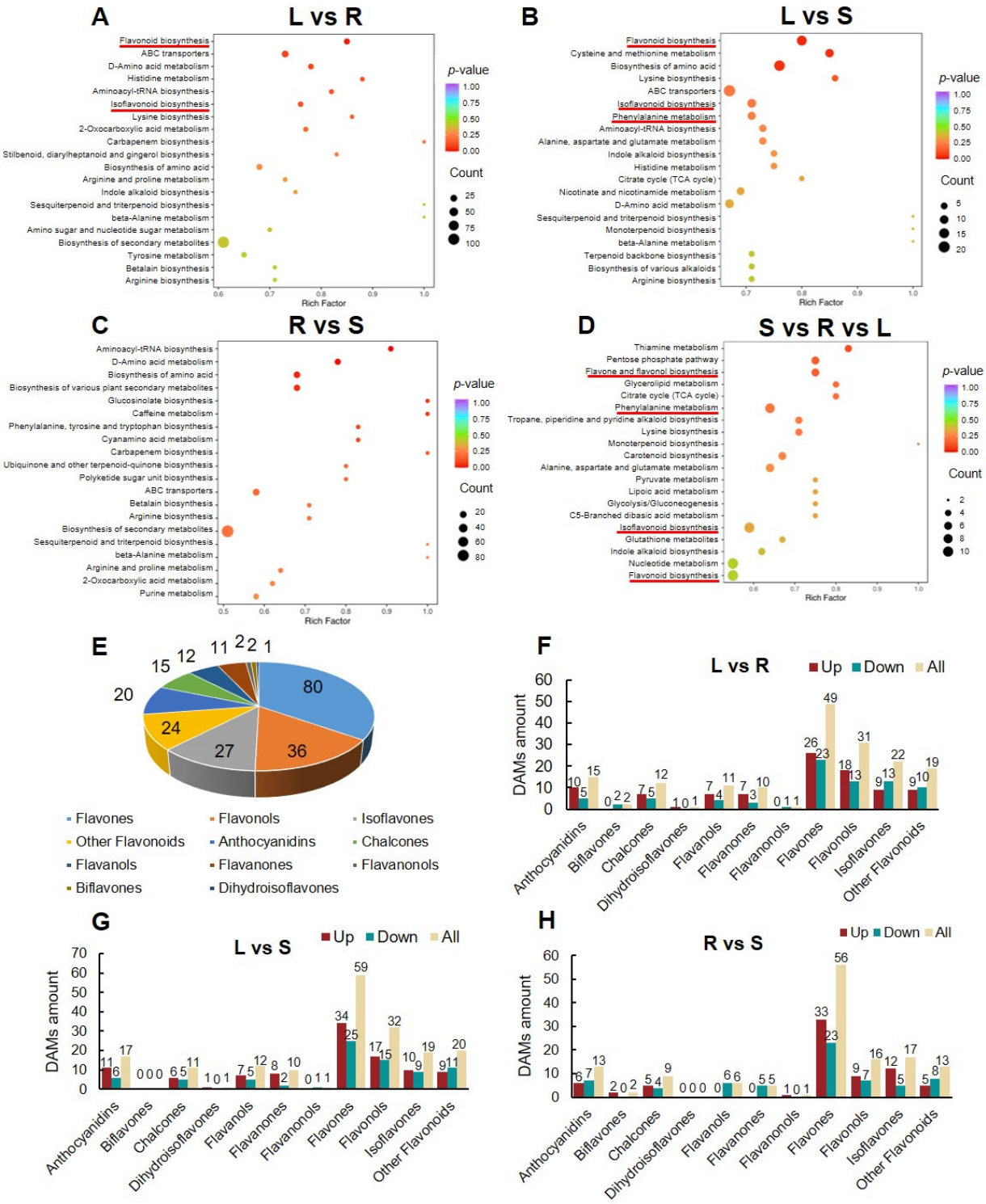


Figure 4. Numbers and categories of DAMs enriched in different compared groups of *S. suberectus* ((**A**–**D**) KEGG pathway enrichment analysis among different compared groups; the red underlines indicate the important pathways related to the metabolism of phenylpropanoids and flavonoids. The red underlines indicated the important pathways related to the metabolism of phenylpropanoids and (iso) flavonoids; (**E**) numbers and categories of flavonoid-related DAMs in *S. suberectus*; (**F**) different flavonoid DAM numbers in the L vs. R group; (**G**) different flavonoid DAM numbers in L vs. S group; (**H**) different flavonoid DAM numbers in the R vs. S group).

As for flavones, 26, 34, and 33 of them were up-regulated in the three compared groups (L vs. R, L vs. S, and R vs. S; same below), while 23, 25, and 23 DAMs were down-regulated. A total of 19 of them appeared in all three compared groups (including (+)-catechin 7-O-beta-D-xyloside, 3′,4′-dimethoxyflavone, 4′-methoxyflavone, chrysin, chrysosplenol D, datiscetin, isochamaejasmin, isoscutellarein, L-epicatechin, nevadensin, oroxylin A, rubraflavone B, taxifolin 3-O-acetate, and so on). For flavonols, 18, 17, and 9 DAMs were up-regulated among all the compared groups, while 13, 15, and 7 DAMs were down-regulated. Five of them were found in all the groups ((+)-catechin gallate, (−)-epiafzelechin, (−)-epicatechin gallate, cianidanol and (+)-gallocatechin). For isoflavones, 9, 10, and 12 DAMs up-regulated, while 13, 9, and 5 DAMs were down-regulated. Seven of them (3,9-dihydroxypterocarpan, 8-O-methylretusin, gancaonin D, glabrone, genistein, pseudobaptigenin, and isoformononetin) were found in all the groups. For anthocyanidins, 10, 11, and 6 DAMs were up-regulated, while 5, 6, and 7 DAMs were down-regulated. Eight of them were found in all the groups (including cyanidin 3-sambubioside 5-glucoside, petunidin 3-galactoside, peonidin chloride, delphinidin 3-sambubioside, leucodelphidin, peonidin pentose, and so on). For chalcones, 7, 6 and 5 DAMs up-regulated, while 5, 5 and 4 DAMs were down-regulated. Five of them were found in all the groups (cardamonin, xanthohumol, pinostrobin chalcone, neohesperidin dihydrochalcone and isoliquiritigenin) (Figure 4F–H, and Supplementary Table S5).

3.2. Transcriptome Analysis Results

(1) Basic sequencing results in all vegetative organs

A total of 449,569,220 clean reads (67.43 Gb high-quality sequences) could be sequenced from the roots, stems, and leaves of *S. suberectus* after a high-quality RNA-seq evaluation and data filtering (6.59~8.45 Gb per sample, Supplementary Table S6). There were also high correlations and good reproducibility (reliability) between different biological replicates and organs (the correlation coefficients ranged from 0.78 to 0.99), especially in the same organ (Supplementary Figure S2). Among the top five most similar plant species of unigenes, 92.67% were highly similar to *Spatholobus suberectus*, 1.70% to *Glycine max*, 1.31% to *Cajanus cajan*, 1.13% to *Mucuna pruriens* and 0.96% to *Glycine soja*, respectively (Figure S3A). All of them belonged to the Fabaceae family, indicating that the transcriptomic characteristics of different organs in *S. suberectus* were similar to those of Fabaceae family species. As for transcription factors (TFs), MYB, bHLH, AP2/ERF-ERF, C2H2, and WRKY were dominant (7.1%, 6.82%, 6.58%, 5.58% and 4.03%, respectively) (Figure S3B). In addition, all the unigenes were divided into 25 types in the KOG database. There were the highest numbers of genes in general function prediction only, posttranslational modification, protein turnover, chaperones and signal transduction mechanisms, respectively (up to 3554, 1962 and 1917), which revealed that signal transduction and some other metabolic processes were important throughout all the organs (Figure S3C).

(2) Differences in gene expression patterns among all vegetative organs and enrichment analysis

There were 15,528 up-regulated DEGs and 13,487 down-regulated DEGs (totaling 29,015) identified in the roots, stems, and leaves of *S. suberectus* (compared with each pair of organs), and 2463 DEGs could be found in all the compared groups between different organs (Figure 5A,B). According to the heatmap, the roots, stems, and leaves were divided into the same cluster, and leaves were alone in another one. DEG numbers in L vs. R were similar to the metabolomics analysis results (Figure 5C). Broken line graphs (Figure 5D) show that in subclasses 3, 4 and 5, roots had the highest gene abundance; in subclasses 1, 2, and 7, leaves had the highest gene abundance, while stems were dominant in the remaining subclasses (Figure 5D). In summary, leaves had more different characteristics

than roots and stems when comparing, and the transcriptome characteristics of the same organs were similar.

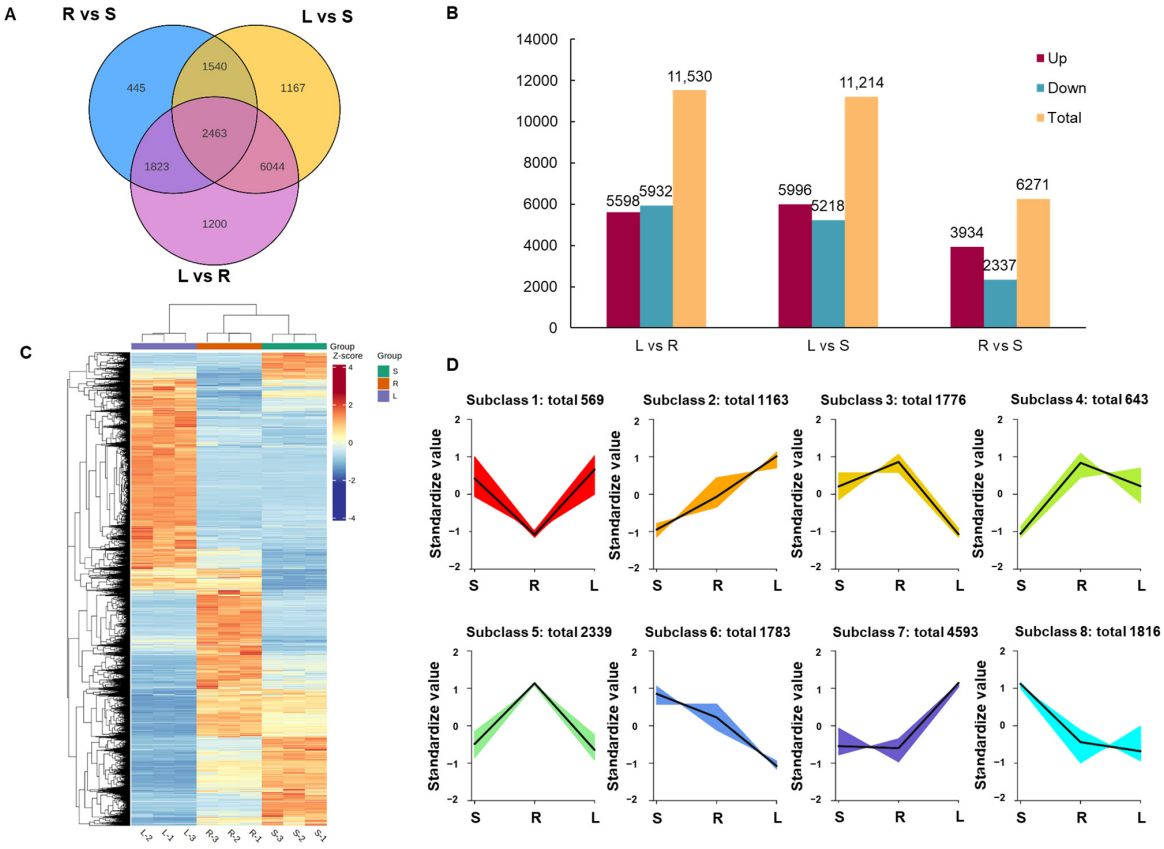


Figure 5. Numbers and cluster analysis of DEGs among different vegetative organs of *S. suberectus* ((**A**) Venn diagram of the shared and unique DEGs among roots, stems and leaves; (**B**) numbers of up-regulated and down-regulated DEGs between different organs comparisons; (**C**) hierarchical clustering analysis of the identified DEGs across three different organs; the horizontal axis represents the sample clusters, and colors from blue to red indicate gene expression levels from low to high; (**D**) the expression trends of the identified DEGs; gene abundance was expressed as $\log_2$-fold change (*y*-axis), and developmental stages are outlined on the *x*-axis, with the S1 stage as the zero point).

(3) Identification analysis of some key pathways and secondary metabolites related to different DEGs (including TFs)

In the KEGG enrichment pathways, biosynthesis of secondary metabolites and metabolic pathways were predominant in all compared groups. It can also be seen that phenylpropanoid biosynthesis and some other pathways about secondary metabolite biosynthesis (such as flavonoid, isoflavonoid, etc.) were also significant through the three compared groups (Figure 6A–C). According to the results of DEG analysis, we focused on the analysis of the relevant pathways of phenylpropanoid and (iso)flavonoids. A total of 362 DEGs (135, 118, and 109 DEGs in L vs. R, L vs. S and R vs. S groups, respectively; same below) were involved in the phenylpropanoid biosynthesis pathway, and 162, 157 and 63 DEGs were detected in the flavonoid biosynthesis (56, 54, and 52, totaling 162), anthocyanin biosynthesis (5, 5, and 3, totaling 13), isoflavonoid biosynthesis (54, 59, and 44, totaling 157), flavone and flavonol biosynthesis pathways (21, 20, and 22, totaling 63), respectively (Supplementary Table S7). In the phenylpropanoid biosynthesis pathway (ko00940), 122 DEGs were up-regulated and 102 DEGs were down-regulated, while 15 up-regulated DEGs and 11 down-regulated DEGs could be found in all compared groups [novel.1895 (*STOX*, encoding tetrahydroberberine ox-

idase), novel.104 (*BBE21*, encoding berberine bridge enzyme-like 21), E2542_SST27339 (*BBE22*, encoding berberine bridge enzyme-like 22), E2542_SST20781 (*CER2*, encoding protein ECERIFERUM 2), E2542_SST20296 (*F5H*, encoding ferulate-5-hydroxylase), E2542_SST16983 (*AOMT*, encoding flavonoid 3′,5′-methyltransferase), E2542_SST13543 and E2542_SST09375 (*3UFGT*, encoding UDP-glucose flavonoid 3-O-glucosyltransferase 5), E2542_SST12919 (*PER55*, encoding peroxidase 55), E2542_SST10720 (*PAR1*, encoding phenylacetaldehyde reductase), E2542_SST10068 (*CCL7*, encoding probable CoA ligase CCL7), E2542_SST08576 (*PER1*, encoding cationic peroxidase 1), E2542_SST01065 (*CCR1*, encoding cinnamoyl-CoA reductase 1), E2542_SST00841 (unknown), and E2542_SST00181 (*PER2*, encoding cationic peroxidase 2) were up-regulated], while 11 DEGs were down-regulated (E2542_SST29328 (*C4H*, encoding cinnamic acid 4-hydroxylase), E2542_SST29260 (*CCR1*, encoding cinnamoyl-CoA reductase 1), E2542_SST29259 (*PAR1*, encoding phenylacetaldehyde reductase), E2542_SST28874 (*SAT*, encoding stemmadenine O-acetyltransferase), E2542_SST27832 (*PER31*, encoding peroxidase 31), E2542_SST23116 and E2542_SST23115 (*PAL2*, encoding phenylalanine ammonia-lyase 2), E2542_SST16680 (*BBE13*, encoding berberine bridge enzyme-like 13), E2542_SST12697 (*PER44*, encoding peroxidase 44), E2542_SST06936 (*PER50*, encoding peroxidase 50), and E2542_SST06588 (*PER64*, encoding peroxidase 64)]. In the flavonoid biosynthesis pathway (ko00941), 49 DEGs were up-regulated and 47 DEGs were down-regulated, and seven DEGs were both up-regulated and down-regulated in the different comparison groups [novel.896 (*6DCS*, encoding NAD(P)H-dependent 6′-deoxychalcone synthase), novel.1325 (*ANR*, encoding anthocyanidin reductase), E2542_SST29615 (*JOX2*, encoding jasmonate-induced oxygenase 2), E2542_SST20781 (*CER2*, encoding protein ECERIFERUM 2), E2542_SST19452 (*F3′H*, encoding flavonoid 3′-hydroxylase), E2542_SST16983 (*FAOMT*, encoding flavonoid 3′,5′-methyltransferase), and E2542_SST01834 (*6DCS*, encoding NAD(P)H-dependent 6′-deoxychalcone synthase) were up-regulated, while novel.872 and novel.3355 (*CHS*, encoding chalcone synthase), E2542_SST29328 (*C4H*, encoding cinnamic acid 4-hydroxylase), E2542_SST28874 (*SAT*, encoding stemmadenine O-acetyltransferase), E2542_SST14749 (*DFR*, encoding dihydroflavonol 4-reductase), E2542_SST07181 (*LDOX*, encoding leucoanthocyanidin dioxygenase), and E2542_SST05681 (*LAR*, encoding leucoanthocyanidin reductase) were down-regulated]. In the anthocyanin biosynthesis pathway (ko00942), two DEGs were up- and down-regulated in three compared groups, and one key DEG could be found in all the groups [E2542_SST17031 (*MdPh-4′-OGT*, encoding phloretin 4′-O-glucosyltransferase) and E2542_SST16525 (*F3GT*, encoding flavonol 3-O-glucosyltransferase)]. In the isoflavonoid biosynthesis pathway (ko00943), 84 DEGs were up-regulated and 47 DEGs were down-regulated (with no DEGs appearing in all three groups). In ko00944, 25 DEGs were up-regulated and 16 DEGs were down-regulated. Three DEGs were up-regulated [E2542_SST26235 (*3AT2*, encoding coumaroyl-CoA), E2542_SST19452 (*F3′H*, encoding flavonoid 3′-hydroxylase) and E2542_SST07938 (*PMAT1*, encoding phenolic glucoside malonyltransferase)] and only one DEG was down-regulated [E2542_SST27635 (*PMAT1*, encoding phenolic glucoside malonyltransferase)] in all three groups (Supplementary Table S7). It can be speculated that the difference in flavonoid biosynthesis and content in *S. suberectus* may be related to the regulatory genes of a series of related enzyme syntheses during the biosynthesis process (*F5H*, *C4H*, *PAL*, *ANR*, *CHS*, *DFR*, *F3′H*, etc.).

Specifically, 382 TF-related DEGs belonging to some TFs related to flavonoid biosynthesis regulation were identified, including MYB (MYB transcription factors, 89), bHLH (basic helix–loop–helix transcription factor, 80), AP2/ERF-AP2 (APETALA2/ethylene responsive factor, 104), WRKY (WRKY transcription factors, 71), and bZIP (basic leucine zipper transcription factors, 38). In roots, there were 42, 42, 35, 22, and 19 genes related to MYB, AP2/ERF-AP2, bHLH, WRKY and bZIP TFs, respectively, and *SsMYB78* (E2542_SST23954),

SsERF72 (E2542_SST01304), *SsbHLH25* (E2542_SST06996), *SsWRK11* (E2542_SST18915), and *SsBZIP9* (E2542_SST15319) had the highest FPKM (Fragments Per Kilobase of exon model per Million mapped fragments) value. In stems, there were 40, 35, 21, 8, and 7 genes related to AP2/ERF-AP2, MYB, bHLH, bZIP and WRKY TFs, respectively, and *SsERF72* (E2542_SST01304), *SsMYB08* (E2542_SST11090), *SsBHLHW* (E2542_SST24136), *SsbZIP44* (E2542_SST10476) and *SsWRK11* (E2542_SST18915) had the highest FPKM value. In leaves, there were 42, 24, 22, 22, and 11 genes related to WRKY, bHLH, MYB, AP2/ERF-AP2 and bZIP TFs, respectively, and *SsWRK11* (E2542_SST18915), *SsBHLHW* (E2542_SST24136), *SsMYB73* (E2542_SST14915), *SsDRE1A* (E2542_SST31394) and *SsTGA2.1* (E2542_SST12562) had the highest FPKM value. In summary, MYB, AP2/ERF-AP2 and WRKY-related genes were dominant in roots, stems and leaves. *SsERF72*, *SsWRK11* and *SsBHLHW* were highly expressed in at least two vegetative organs (Supplementary Table S8).

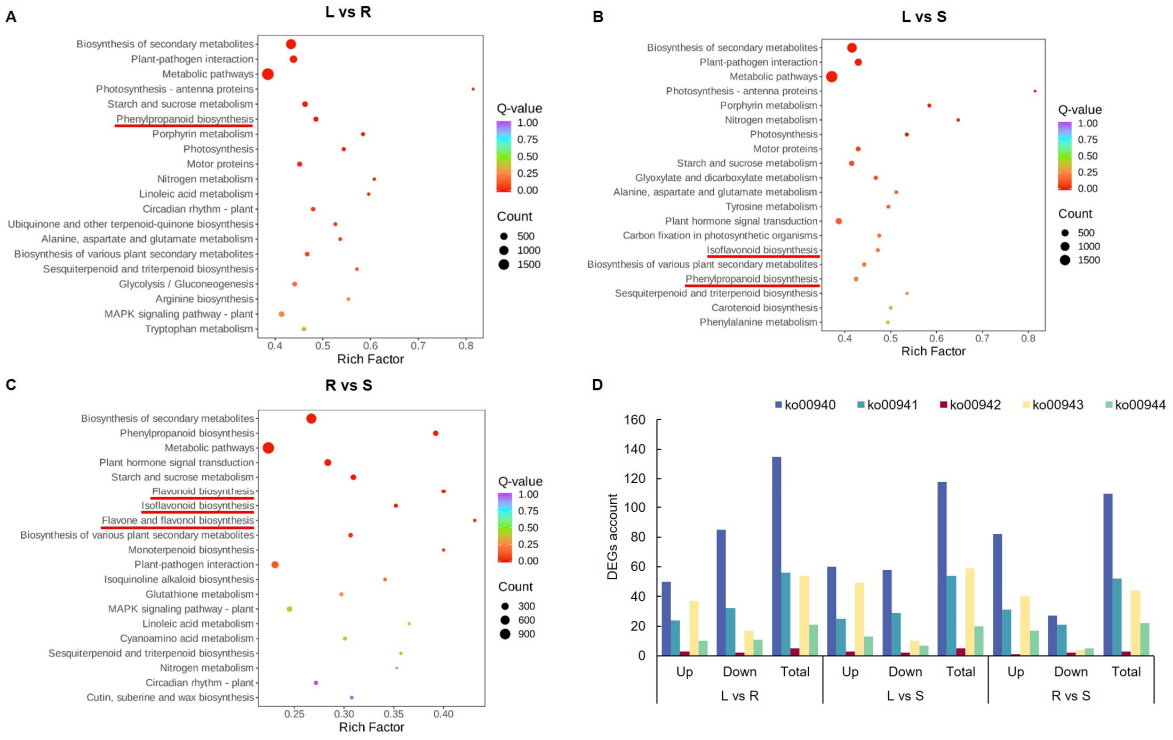


Figure 6. Numbers and cluster analysis of DEGs among different vegetative organs of *S. suberectus* ((**A**–**C**) KEGG enrichment analysis among different compared groups of *S. suberectus;* the red underlines indicate the important pathways related to the metabolism of phenylpropanoids and flavonoids. The red underlines indicated the important pathways related to the metabolism of phenylpropanoids and (iso) flavonoids; (**D**) numbers of up-regulated and down-regulated DEGs between different organ comparisons).

3.3. Integrated Analysis

3.3.1. WGCNA Analysis for Different Vegetative Organs of *S. suberectus*

WGCNA analysis was conducted based on the genes throughout different organs (roots, stems, and leaves) of *S. suberectus* (Figure 7 and Supplementary Tables S9–S11). A soft-thresholding power of β = 18 was selected based on the scale-free topology fit index ($R^2 > 0.8$). The numbers of genes in turquoise and blue modules were the highest (6849 and 4971, respectively). There were many related unigenes in the blue module for stems (correlation coefficients ranged from 0.46 to 0.48), in the yellow module for roots (correlation coefficients ranged from 0.49 to 0.51) and in the turquoise module for leaves (correlation coefficients ranged from 0.49 to 0.51) (Figure 7C). In the blue module, there were 25, 23, 1, 5, and 6 unigenes, which belonged to the five main pathways of flavonoid

biosynthesis (ko00940, ko00941, ko00942, ko00943 and ko00944; same below). TF-related genes of C2H2, MYB, bHLH, NAC and C3H were the highest. In the yellow module, 47, 17, 1, 10 and 9 unigenes belonged to these pathways, respectively, and the related genes of MYB, bHLH, C2H2, bZIP and WRKY were dominant. In the turquoise module, 54, 18, 3, 34, and 8 unigenes belonged to these pathways, respectively, and the related genes of WRKY, bHLH, MYB, NAC and C2H2 were dominant among all the TF-related genes. Phenylalanine ammonia-lyase 1 (*PAL1*), phenylalanine ammonia-lyase 2 (*PAL2*), 4-coumarate-CoA ligase 2 (*4CL2*), flavonol synthase (*FLS*), bifunctional dihydroflavonol 4-reductase (*DFR*), flavonol 3-O-glucosyltransferase (*F3GT2*), flavonoid 3′-monooxygenase (*F3′H*) and many other genes were dominant and closely related to flavonoid biosynthesis, encoding key enzymes during the flavonoid biosynthesis process. The FPKM values of most these unigenes followed the trend of stems>leaves>roots, and some genes related to anthocyanidin biosynthesis (such as anthocyanidin 3-O-glucosyltransferase, *UFGT* and UDP-glycosyltransferase, *UGT13*, cyanidin 3-O-galactoside 2″-O-xylosyltransferase, *UFGT6b*) were also highly expressed in stems and leaves, which were related to some specific anthocyanidin contents. In addition, some TF-related unigenes (*MYB*, *bHLH*, *WRKY*, *APR*, etc.) were also highly expressed in stems compared to roots and leaves (Supplementary Tables S9–S11). In summary, the unigenes encoded key enzymes related to flavonoid biosynthesis, and some related genes of MYB, bHLH, AP2/ERF-AP2, and WRKY were important among all the vegetative organs of *S. suberectus*, and they also had the functions of regulating the biosynthesis of flavonoids, flavonols/flavones, isoflavonoids and some other secondary metabolites among most medicinal plants.

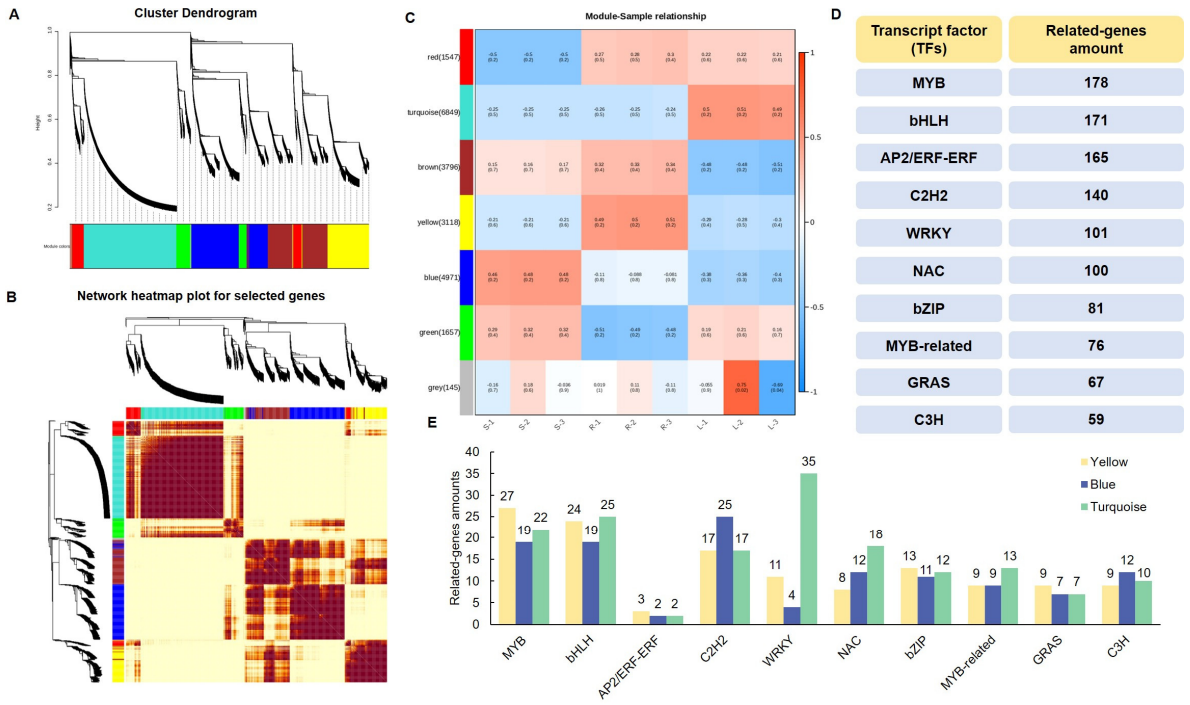


Figure 7. Weighted gene coexpression network analysis (WGCNA) of the identified genes between roots, stems, and leaves of *S. suberectus* ((**A**) gene dendrogram obtained by clustering the dissimilarity based on consensus topological overlap, with each tree branch constituting a module and each leaf representing one gene; each colored row indicates a color-coded module that contains a group of highly interconnected genes; (**B**) heatmap plot of topological overlap in the gene network; darker squares along the diagonal correspond to modules; (**C**) module eigengene physiological indexes and sample correlations; the color scale bar on the right shows the correlation range from negative to positive; (**D**) total numbers of unigenes in all the vegetative organs of *S. suberectus*; (**E**) main TF-related genes among blue, yellow, and turquoise modules).

3.3.2. Integrated Analysis of Transcriptomics and Metabolomics Between Different Vegetative Organs

To indicate the correlations between specific DAMs (including phenylalanine and the main phenolic acid, (iso)flavonoid) and DEGs encoding key enzymes during the process of phenylpropanoid and (iso)flavonoid biosynthesis among different vegetative organs and flavonoid-related pathways of *S. suberectus*, we used Pearson's correlation coefficient analysis to find the relationships between them (choosing those with a correlation value larger than 0.8 and a significance level of $p < 0.05$, Figure 8). Spearman's rank correlation was used to assess gene–metabolite relationships. Given the limited sample size (n = 3 per organ), *p*-values were adjusted using the Benjamini–Hochberg false discovery rate (FDR) method. Correlations with $|r| > 0.8$ and $p < 0.05$ were considered significant. These results are exploratory and require validation. Most of these DEGs in the different pathways were closely connected with their corresponding flavonoids, suggesting coordinated regulation between gene expression and metabolite accumulation (detailed information of flavonoids and unigenes is shown in Supplementary Table S12). In the phenylpropanoid biosynthesis pathway (ko00940), *PAL*, *3GT5*, *4CL* and some other genes showed positive correlations with L-phenylalanine and some other phenolic acids; in the flavonoid biosynthesis pathway (ko00941), the expressions of *CHS* and *DFR* showed positive correlations with naringenin, (+)-gallocatechin, epigallocatechin, (−)-epiafzelechin and many other compounds, while the expressions of *ANR* showed negative correlations many flavonoids. Chrysin showed negative correlations with many genes (*F3′H*, *FLS*, *CHS*, etc.), and *FLS1/FLS3* also showed negative correlations many flavonoids (such as sakuranetin, naringin, and so on). For cyanidin 3-sambubioside 5-glucoside (a kind of anthocyanin), *FGT* and *KGLT* showed positive correlations with it, while *F3GT2* showed the opposite. Interestingly, *ANR1* (E2542_SST11123), and *ANR2* (novel.1325) always showed the opposite trend among most of the flavonoids. In the isoflavonoid biosynthesis pathway (ko00943), *VESTR* and *C81E1* showed positive correlations with most of the flavonoids (except for 6″-O-malonylglycitin, formononetin, ononin, pseudobaptigenin and isoformononetin), and *I2′H/IFR* showed a similar trend (except for 6″-O-malonylglycitin, ononin, and isoformononetin). 2′-Hydroxydaidzein, 5-hydroxypseudobaptigenin, genistein, coumestrol, and naringenin showed positive correlations with most of the genes except for *UGT2*, while 6″-O-malonylglycitin, formononetin, ononin and isoformononetin showed negative correlations with most of the genes except for *UGT2*. Daidzein and glycitein both showed positive correlations with the *I2′H*, *I3′H*, *IFR*, and *UGT1* genes. For flavone and flavonol biosynthesis, *F3GGT* showed positive correlations with meloside A, luteolin and 3,7-Di-O-methylquercetin, while it showed negative correlations with myricetin (with *F3′5′H*). Notably, up-regulation of *PAL*, *4CL*, *C4H*, *CHS*, *DFR*, and some other genes would cause the biosynthesis of many flavonoids, and up-regulated expression levels of *C81E1*, *C81E9*, *IFR*, *UGT1* would promote isoflavonoid biosynthesis. Some key genes selected from the blue modules of WGCNA with high expression levels, like *PAL1* (E2542_SST12001), *PAL2* (E2542_SST24497), *4CL2* (E2542_SST07412), *CHS* (E2542_SST12829, novel.872), *DFR* (E2542_SST14749), *F3′H* (E2542_SST02067, E2542_SST02070, E2542_SST02071), *LAR* (E2542_SST05681), and *UGT2* (E2542_SST31584), are also important during this process. In addition, some genes related to lignin synthesis and cell wall formation (*CAD*, *CCR*, *COMT1*, *CSE*, *SNL6*, *WAK2*, etc.) were also significantly enriched and correlated in the phenylpropanoid pathway, which might be highly correlated with flavonoid biosynthesis. These results reveal the complex regulatory process of (iso)flavonoid biosynthesis in vegetative organs.

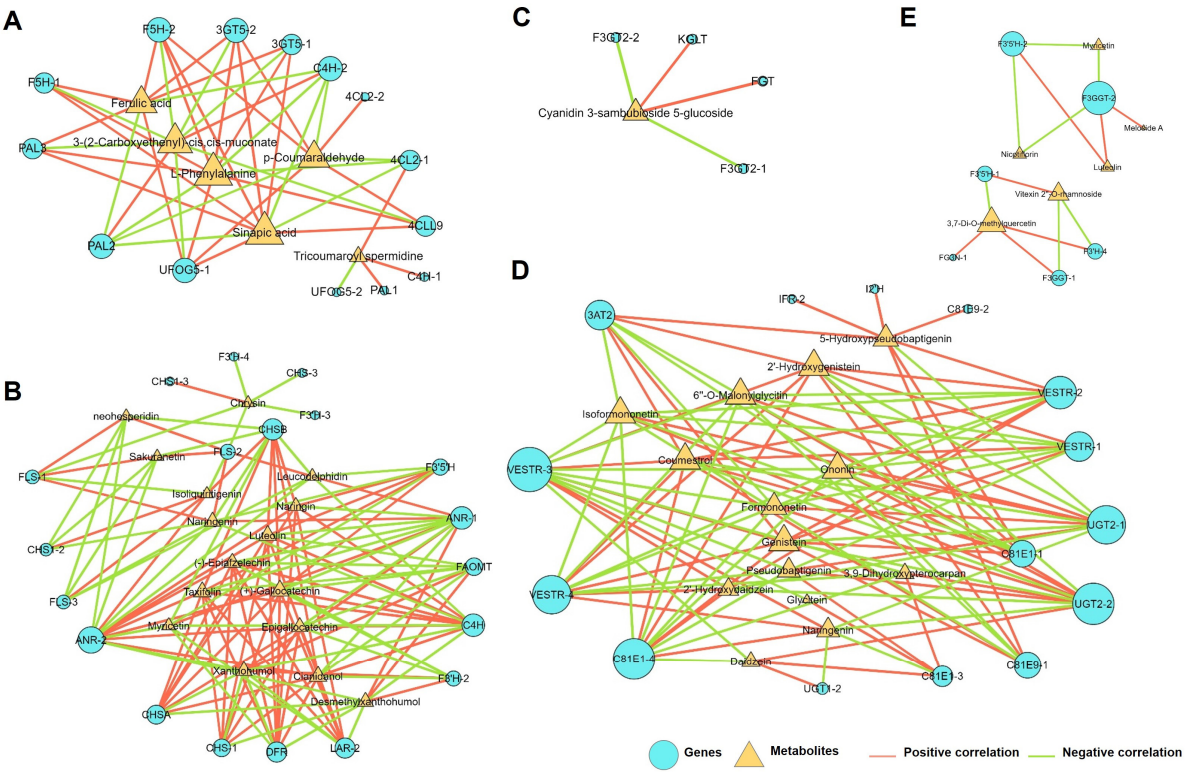


Figure 8. Correlation analysis of genes and key flavonoid metabolites in different pathways of *S. suberectus* ((**A**) ko00940: phenylpropanoid biosynthesis; (**B**) ko00941: flavonoid biosynthesis; (**C**) ko00942: anthocyanin biosynthesis; (**D**) ko00943: isoflavonoid biosynthesis; (**E**) ko00944: flavone and flavonol biosynthesis).

3.3.3. Flavonoid Biosynthesis Characteristics in *S. suberectus*

The biosynthesis of (iso)flavonoids in *S. suberectus* is complicated (Figure 9). At the beginning of the ko00940 pathway, the phenylalanine content was highest in leaves, followed by roots and stems, but the expression of *PAL* was higher in stems than in roots and leaves. *F5H* in this pathway was highly expressed in leaves, causing high contents of some phenolic acids. For ko00941 (flavonoid biosynthesis pathway), *CHS* and *CHI* had high expression levels in stems, and the contents of chalcones and some flavanones were high in stems compared to roots and leaves. The expression levels of *F3′H*, *DFR*, *ANS*, and *LAR* were also high in stems, and (+)-catechin mainly accumulated in stems, but the contents of some other anthocyanins (like pelargonidin and cyanidin) were higher in leaves. In the isoflavonoid biosynthesis pathway (ko00943), *I2′H* and *I3′H* were highly expressed in leaves, causing an improvement in 2′-hydroxygenistein content, but on the contrary, *UGT2* had high expression levels in stems. Ononin, isoformononetin, 6″-O-malonylglycitin, and some other components were abundant in stems. In the ko00944 pathway, the expression levels of *F3H* and *F3′H* were high in stems and leaves, but *F3′5′H* was abundant in roots. Notably, most of the flavonol contents were high in leaves, indicating that there were negative correlations between the expression of these genes and flavonol contents. In general, genes from the phenylpropanoid and flavonoid biosynthesis pathways and some genes from the anthocyanin biosynthesis pathway (like *DFR*, *ANS*, *ANR*, and *LAR*) were highly expressed in stems compared to roots and leaves, but genes in the flavone and flavonol biosynthesis pathways (like *F3′5′H*) showed the opposite trend. Flavones and isoflavonoids were abundant in stems and roots, while phenolic acids/some anthocyanins/flavonols were abundant in leaves.

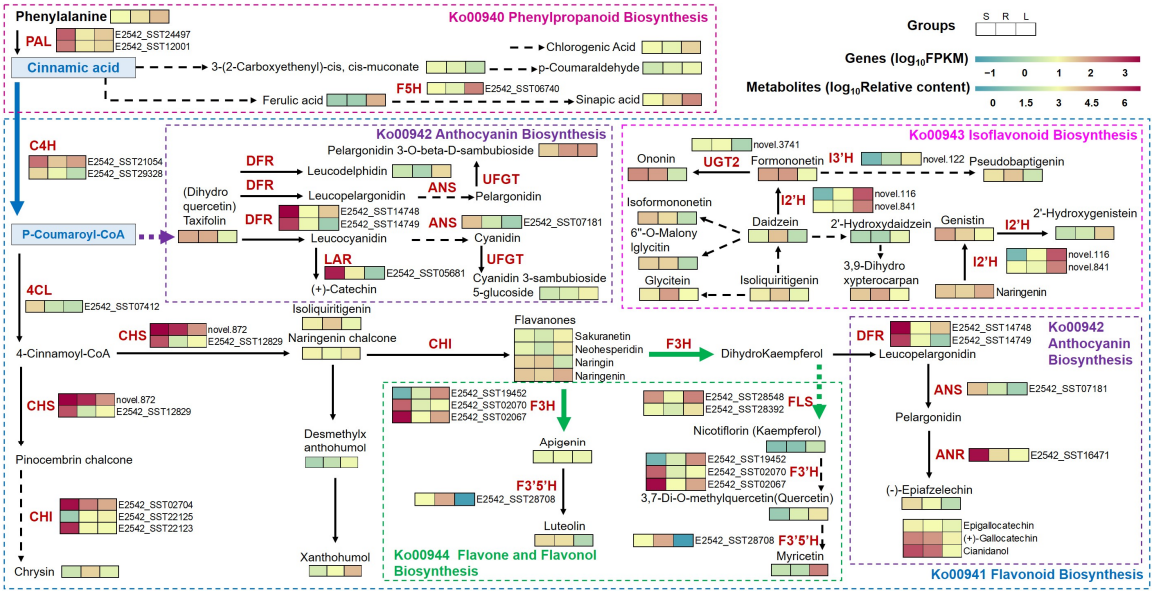
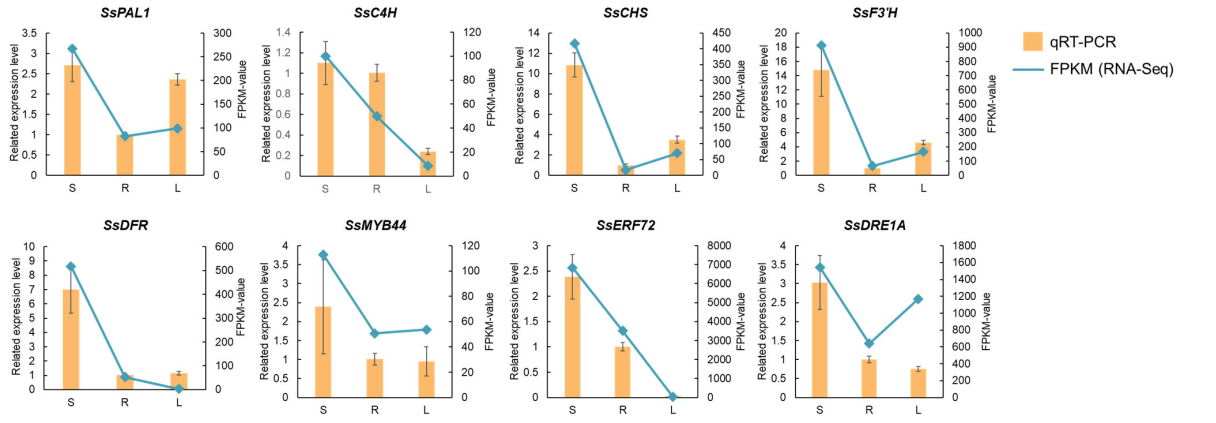


Figure 9. Pathway network of differentially expressed genes (DEGs) and differentially accumulated metabolites (DAMs) involved in the flavonoid and phenylalanine biosynthesis pathways among all the vegetative organs of *S. suberectus.* Heatmaps in this figure show the FPKM values of DEGs and relative content values of DAMs after $\log_{10}$ transformation.

3.3.4. qRT-PCR Results

Eight representative DEGs encoding key enzymes and transcription factors (with high expression levels and different FPKM values in all the vegetative organs) were chosen for qRT-PCR analysis from all the compared groups and WGCNA modules (Figure 10 and Supplementary Table S13). We chose *SsACT* (E2542_SST27345) as the reference gene (due to its steady expression in all vegetative organs). It was found that the expression trends of different genes were the same as the FPKM results of RNA-seq. So, the transcriptome data could be used to reflect transcript abundance in this study.



GeneID	Gene	FPKM-value			Primer information		Product size	GeneID	Gene	FPKM-value			Primer information		Product size
		S	R	F	Type	sequence(5'-3')				S	R	F	Type	sequence(5'-3')	
E2542_SST12001	*SsPAL1*	266.81	82.74	99.30	F	TAATGGCACGGCTGTTGGTT	118 bp	E2542_SST02067	*SsF3'H*	913.26	67.09	165.81	F	TGGCCCATAGTGGGAAACCT	184 bp
					R	AGGTTTCCCTTGCATCACTTCA							R	GCCGGCTGCTGAAATTAGAGT	
E2542_SST29328	*SsC4H*	100.05	49.76	8.56	F	GGGCTATGACATCCCTGCTGA	142 bp	E2542_SST06907	*SsMYB44*	112.94	50.64	53.76	F	GCAGAACCGACAACGCAATC	197 bp
					R	ATTCCCATTGGCCTCCACC							R	TACGCTGGACTCGCTCACATC	
E2542_SST12829	*SsCHS*	417.41	17.14	70.50	F	GCCTGAGACCCTCCGTGAAG	127 bp	E2542_SST01304	*SsERF72*	6835.86	3514.17	38.18	F	GAGAAGGGTAACGGAGGGAAGA	137 bp
					R	GAGCAGACGACGAGCACCCT							R	AAGGTGCCGAGCCAGACG	
E2542_SST14749	*SsDFR*	517.58	53.13	3.05	F	TGGCGGAGCAAGAAGCG	102 bp	E2542_SST31394	*SsDRE1A*	1543.75	640.13	1168.63	F	CAGGATTTGGCTGGGGACTT	169 bp
					R	GCAATGTTGGCGTAAGAAAAGG							R	CTCTGCTGCCGCCTTTTGTA	

Figure 10. Gene expression validation of key functional enzymes and transcription factor genes involved in flavonoid biosynthesis in different vegetative organs of *S. suberectus* using a qRT-PCR assay. The data are presented as means of three replicates, and error bars denote ±SE (n = 3).

4. Discussion

4.1. Flavonoid and Metabolite Contents in All the Vegetative Organs of S. suberectus

Previous studies showed that dried vine stems of *S. suberectus* have always been used for ethnomedicine [31], but in this study, we found that flavonoids, amino acids (and their derivatives) and alkaloids/terpenoids followed the rule of stems>leaves>roots, leaves>stems>roots and roots>leaves>stems, respectively, a result which is similar to various medicinal plants and also consistent with our hypothesis about *S. suberectus*. This pattern aligns with the general roles of flavonoids as aboveground stress protectants (UV, pathogens, herbivores), while alkaloids/terpenoids in underground parts could be used to defense against multiple stresses [8,32]. Similarly, the biosynthesis of flavonoids helps plants defend against *Botrytis cinerea* or other pathogens, and it helps stems avoid damage caused by UV-B, cold and other stresses [8,33,34]. Grapes [10], *Hippophae rhamnoides* (kaempferitrin [35]) and many other woody plants had high flavonoid accumulation levels in their stems and bark; proanthocyanins, epicatechin, catechin, kaempferol 3-O-glucoside and many other flavonoids were the main components in vines and berry stems of *Vitis davidii* [36]. In summary, flavonoids always accumulate more in aboveground parts than underground parts as an important antioxidant for stress defenses. As for alkaloids and terpenoids, roots were the main organ which produced them. They synthesized in the underground parts and exported to the shoots via phloem and function as a chemical barrier against herbivores and pathogens [37,38]. In this study, *S. suberectus* was planted under a *Pinus elliottii* forest for 6 years, and the roots needed to contend with various microorganisms in the soil. This might be the possible reason why alkaloids and terpenoids mainly accumulated in the roots of *S. suberectus*. In summary, all the vegetative organs of *S. suberectus* had abundant chemical components that could be used adequately after oriented cultivation.

4.2. Biosynthesis of Specific Flavonoid Metabolites Among All the Vegetative Organs of S. suberectus

Flavonoids consist of various categories (flavones, flavonols, chalcones, anthocyanins, etc.), and flavones were dominant [39]. For *S. suberectus*, we found that flavonoids mainly accumulated in stems, while anthocyanins/chalcones mainly accumulated in leaves, which is consistent with various medicinal plants. Previous phytochemical studies on *S. suberectus* have mainly focused on its medicinal values and some component properties, but the organ-specific distribution of different flavonoid subclasses (flavones, flavonols, anthocyanins) across roots, stems, and leaves has not been systematically compared. Notably, we found that there were different numbers of red stem rings on cross-sections of *S. suberectus* stems (Figure 1B). Some specific anthocyanins (like pelargonidin, delphinidin and peonidin) also had high contents. Similarly, pelargonidin in *Paeonia* [40] and *Rosa rugosa* [41] and peonidin in *Cymbidium ensifolium* [42] and *Torenia fournieri* [43] were the main pigments that made the tissues show pink and red colors. Anthocyanins can be found in dark-colored flowers or plant tissues. Pelargonidin and delphinidin always show purple–pink colors, while peonidin always shows a dark red coloration in plant tissues. Their contents showed close relationships with DFR, ANS and other enzymes (also related to genes encoding them). For example, the peonidin content was regulated by the expression of *DFR*, *FLS*, and some other genes in *Prunus mume* stems [44], the expression of *F3′5′H* regulated the biosynthesis of *Capsicum annuum* stems [45], and the expression of *CHI1*, *ANS*, and other key genes influenced the color of *Panax notoginseng* via the pelargonidin-3-O-[-3′′-(-2′′′-O-malonyl)-α rhamnosyl]-β-xyloside content [46]. All of them showed a dark red or purple color. In summary, flavones/flavonols were the main categories of flavonoids, while the contents of

pelargonidin, delphinidin, and peonidin mainly influenced the degree of the purplish–red cross-section of the stem (rings).

4.3. The Expression of Key Enzyme Genes Among All the Vegetative Organs During the Flavonoid Biosynthesis Process of S. suberectus

In our study, 4040 DAMs and 29,015 DEGs were identified from all the vegetative organs, and flavonoid-related DAMs and DEGs played significant roles. Stems and roots were in the same cluster in both transcriptomic and metabolomic analyses, while leaves formed a separate cluster, indicating that leaves had more different metabolites and genes than roots and stems. This result was similar to *Ormosia henryi* [47], *Scutellaria baicalensis* [48] and some other medicinal plants. Therefore, there is a large gap between the chemical components in the leaves of *S. suberectus* and those in the roots and stems.

The characteristics of flavonoid-biosynthesis-related pathways (ko00940, ko00941, ko00942, ko00943, and ko00944) were deeply analyzed. At the beginning of the flavonoid biosynthesis process (from ko00940 to ko00941), phenylalanine was an important precursor in the primary biosynthesis stage, which showed high correlations with PAL, C4H, and other key enzymes [8]. Most of their encoding genes showed high expression levels in stems, causing some chalcone and flavone accumulations. For example, *Cs4CL1* expression increased flavonoid accumulation in *Camellia sinensis* stems [49], and the down-regulation of *C4H*, *CHS*, and *CHI* decreased the flavonoid content in *Dioscorea polystachya*. Then, the expression of *CHS* and *CHI* caused an increase in the content of various chalcones, flavones, and flavonols, like pinocembrin chalcone, pinocembrin, naringenin, and so on [50–52]. Isoliquiritigenin and other component contents showed similar trends to the expression levels of *CHS* and other genes in our study. In the anthocyanin biosynthesis pathway (ko00942) of *S. suberectus*, DFR, ANS, and ANR turned dihydrokaempferol into leucopelargonidin, pelargonidin, and catechin after flavanones, with high expression levels of their encoding genes observed in stems, which was similar to that observed in 'Red Meat Honey Crisp (RMHC)' peach [53], *Valeriana jatamansi* [54] and other plants. In the isoflavonoid biosynthesis pathway (ko00943), we could see that I2′H, I3′H and UGT2 catalyzed the synthesis of isoflavones from isoliquiritigenin, naringenin and other substances, which was similar to the results of *Glycine max* [55], *Ginkgo biloba* [56], *C. sinensis* [57], etc. Ononin, isoformononetin and other isoflavonoid contents, as well as the expression levels of *UGT2* and *I2′H,* were higher in stems and roots. In the flavone and flavonol biosynthesis pathway (ko00944), *F3′H* and *FLS* were highly expressed in stems and leaves, causing the accumulation of flavonols, especially myricetin. In *Lycium chinense* [58], *Glechoma longituba* [59] and many other medicinal plants, the expression modes of the *F3′H*, *F3′5′H*, and *FLS* genes were closely related to flavonol contents. In addition, the overexpression of *FLS* in *C. sinensis* leaves caused flavonol (kaempferol, quercetin and myricetin derivatives) accumulation [60]; *FLS*, and *F3′5′H* showed high correlations with myricetin and M-based flavonols in different organs of *Morella rubra* [61]. In summary, the expression levels of most *CHS*, *CHI*, *F3H*, *DFR*, *ANS* and *ANR* genes were high in stems, which showed high correlations with flavanone and flavanol accumulation. The high expression levels of *F3′H* and other genes highly correlated with the accumulation of flavonols, especially myricetin, and others.

We acknowledge that our transcriptomic analysis was performed at the organ level, which represents an average expression profile across all cell types within each organ. Different organs (roots, stems, leaves) have distinct cell type compositions, and cell-type-specific expression patterns may be masked by bulk RNA-seq. Therefore, the observed up- or down-regulated DEGs between organs should be interpreted as organ-level differences. While single-cell or spatial transcriptomics could provide higher resolution, these

approaches are accompanied by technical challenges, with the disadvantages of cell–cell communication loss upon cell isolation, and should be interpreted with caution [62].

4.4. The Expression of Key Transcription Factor (TF) Genes Among All the Vegetative Organs During the Flavonoid Biosynthesis Process of S. suberectus

Transcription factors (TFs) play essential roles in regulating flavonoid biosynthesis [25]. We identified several TFs with markedly high expression levels in stems compared to roots or leaves, including *SsMYB44* (MYB family), *SsbHLH35* (bHLH family), *SsERF72* and *SsDRE1A* (AP2/ERF family), and *SsWRK44* (WRKY family). Their stem-enriched expression suggests potential involvement in the organ-specific regulation of flavonoid accumulation. MYB44, a member of the R2R3-MYB subfamily, has been reported to regulate stress responses and flavonoid biosynthesis in some species [27]. However, its function appears to be species-dependent: it promotes flavonoid accumulation in *Ziziphus* [63,64] but acts as a negative regulator in blueberry and goji (*Lycium barbarum*) berries [65,66]. The high expression of SsMYB44 in *S. suberectus* stems points to a possible role in stem-specific flavonoid synthesis, but its exact regulatory mode requires functional validation. bHLH and AP2/ERF TFs are known to positively regulate flavonoid biosynthesis in many plants by activating structural genes such as *CHS* and *CHI* [67–69]. Similarly, *WRKY* can promote flavonoid accumulation through direct or indirect activation of biosynthetic genes [70], which may also increase phenylalanine and major flavonoid contents [71]. The stem-enriched expression of *Ss*bHLH35, *Ss*ERF72, *Ss*DRE1A and *Ss*WRK44 therefore suggests that these TFs may act cooperatively to drive flavonoid production in *S. suberectus* stems. To sum up, genes related to these specific TFs were closely related to flavonoid biosynthesis regulation and gene expression of key enzymes in most plants. Future studies—such as heterologous expression or gene silencing—are needed to confirm their regulatory functions and to assess their potential for metabolic engineering or marker-assisted breeding of *S. suberectus*.

5. Conclusions

Amino acids and derivatives, flavonoids, and alkaloids/terpenoids were the main secondary metabolites in roots, stems and leaves of *S. suberectus*, respectively. Stems were utilized due to their abundant flavanols, flavonols, flavones, flavanonols, and other flavonoids. In addition, DAMs and DEGs were significantly enriched in the pathways related to phenylpropanoid and (iso)flavonoid biosynthesis. Many genes encoding key enzymes of flavonoid biosynthesis (like *PAL*, *C4H*, *CHS*, *F3′H*, *F3′,5′H*, *DFR*, *ANR*, *LAR*, etc.) and transcription factors (like *ERF72*, *WRK11*, *BHLHW*, etc.) were found in all the compared groups. These key genes were also found in blue, yellow, and turquoise modules for roots, stems and leaves via WGCNA analysis. From an integrated analysis, we found that *PAL*, *4CL*, and some other genes showed positive correlations with L-phenylalanine; *C4H*, *CHS*, *DFR* and some other genes showed positive correlations with various flavonoids, while FLS showed negative correlations with many flavonols and flavonoids. Flavones and isoflavonoids were abundant in stems and roots, while phenolic acids/some anthocyanins/flavonols were abundant in leaves. The results of qRT-PCR showed consistency with the FPKM values of the RNA-seq results, indicating that the results of this study were reliable. In summary, this study provides a new perspective for further understanding the accumulation characteristics of various kinds of active compounds among all the vegetative organs of *S. suberectus*, which lays the foundation for the efficient utilization of different organs of *S. suberectus*.

Supplementary Materials: The following supporting information can be downloaded at: https://www.mdpi.com/article/10.3390/horticulturae12060653/s1, Figure S1. Amounts and PCA analysis

of secondary metabolites among different organs of *S. suberectus*; Figure S2. Pearson's correlation and PCA analysis between different organs and samples of *S. suberectus*; Figure S3. A—Unigene similarity analysis in NR database; B—main transcript factors in roots, stems and leaves of *S. suberectus*; C—results of KOG classification; Figure S4. Melt curves of unigenes of qRT-PCR analysis; Figure S5. Amplification plots of unigenes of qRT-PCR analysis. Supplementary Table S1. HPLC conditions (samples injection details); Supplementary Table S2. MS conditions. Supplementary Table S3. Metabolite counts; Supplementary Table S4. Flavonoid characteristics; Supplementary Table S5. Different expressed flavonoids; Supplementary Table S6. QC and number of reads; Supplementary Table S7. KEGG pathway and DEGs analysis; Supplementary Table S8. Transcription factor genes; Supplementary Table S9. Unigenes in blue module; Supplementary Table S10. Unigenes in yellow module; Supplementary Table S11. Unigenes in turquoise module; Supplementary Table S12. DEGs and DAMs corrrelations; Supplementary Table S13. Genes for qRT-PCR analysis.

Author Contributions: D.M. and D.Y.: writing—original draft, visualization, data curation, investigation, methodology, formal analysis; M.L., J.L., and X.Z.: resources, data curation, writing—review and editing; Y.X. and M.Y.: conceptualization, supervision, project administration, writing—review and editing. D.M. and D.Y. made equal contributions to this work. All authors have read and agreed to the published version of the manuscript.

Funding: (1) Guangxi Science and Technology Base and Talent Project (Guike AD23026191); (2) National Natural Science Foundation of China (32501621); (3) Guangxi Key Research and Development Project (Guike AB21238014); (4) Guangxi University Young and Middle-aged Teachers Research Basic Ability Improvement Project (2023KY0016).

Institutional Review Board Statement: *S. suberectus* was common in the understory environment in Guangxi and Southern China, and it was not included on the IUCN Red List of Threatened Species. The sample collection process was approved by the College of Forestry, Guangxi University, and Guangxi State-Owned Qipo Forest Farm. All the sample collection processes followed ethical guidelines to ensure the normal growth of *S. suberectus* under the *P. elliottii* forest.

Data Availability Statement: The RNA sequencing data reported in this manuscript have been deposited in the Genome Sequence Archive in the National Genomics Data Center, China National Center for Bioinformation/Beijing Institute of Genomics, Chinese Academy of Sciences (submission ID: subSAM155641; project ID: PRJCA050565) and are publicly accessible at https://ngdc.cncb.ac.cn/. In addition, all other relevant data are within the manuscript and the Supplementary Materials.

Acknowledgments: The authors acknowledge the following institutions for supporting this work: (1) College of Forestry, Guangxi University; (2) Key Laboratory of National Forestry and Grassland Administration on Cultivation of Fast-Growing Timber in Central South China; (3) Guangxi Key Laboratory of Forest Ecology and Conservation. Heatmaps in the manuscript were created using Metware Cloud, a free online platform for data analysis (https://cloud.metware.cn). We also thank Siraj Ud Din for his help in language improvement and editing.

Conflicts of Interest: The authors declare that they have no conflicts of interest.

References

1. Chen, H.L.; Yang, J.; Fu, Y.F.; Meng, X.N.; Zhao, W.D.; Hu, T.J. Effect of total flavonoids of *Spatholobus suberectus* Dunn on PCV2 induced oxidative stress in RAW264.7 cells. *BMC Complement. Altern. Med.* **2017**, *17*, 244. [CrossRef]
2. Liu, X.Y.; Zhang, Y.B.; Yang, X.W.; Yang, Y.F.; Xu, W.; Zhao, W.; Peng, K.F.; Gong, Y.; Liu, N.F.; Zhang, P. Anti-Inflammatory Activity of Some Characteristic Constituents from the Vine Stems of *Spatholobus suberectus*. *Molecules* **2019**, *24*, 3750. [CrossRef]
3. Huang, X.J.; Fei, Q.Q.; Yu, S.; Liu, S.J.; Zhang, L.; Chen, X.L.; Cao, L.; Wang, Z.Z.; Shan, M.Q. A comprehensive review: Botany, phytochemistry, traditional uses, pharmacology, and toxicology of *Spatholobus suberectus* vine stems. *J. Ethnopharmacol.* **2023**, *312*, 116500. [CrossRef]
4. Yoon, J.S.; Sung, S.H.; Park, J.H.; Kim, Y.C. Flavonoids from *Spatholobus suberectus*. *Arch. Pharm. Res.* **2004**, *27*, 589–592. [CrossRef] [PubMed]
5. Inami, K.; Asada, Y.; Harada, T.; Okayama, Y.; Usui, N.; Mochizuki, M. Antimutagenic components in *Spatholobus suberectus* Dunn against N-methyl-N-nitrosourea. *Genes Environ.* **2019**, *41*, 22. [CrossRef]

6. Qin, S.S.; Liang, Y.; Wei, G.L.; Wei, F.; Wei, K.H.; Chen, X.Y. Shade responses and resistant mechanisms in *Spatholobus suberectus*. *Heliyon* **2024**, *10*, e28077. [CrossRef] [PubMed]
7. Chen, B.L.; Yang, K.T.; Tang, C.H.; Long, S.Y.; Wang, Y.C.; Wang, Y.W.; Ye, Y.W.; Liu, J. Selection and Comprehensive Evaluation of Ecological Cultivation for 16 Models of Tree-Medicina under Pine Forests in Low Hills of Guangxi. *Guangxi For. Sci.* **2024**, *53*, 819–828. (In Chinese) [CrossRef]
8. Ma, D.C.; Guo, Y.M.; Ali, I.; Lin, J.R.; Xu, Y.Y.; Yang, M. Accumulation characteristics of plant flavonoids and effects of cultivation measures on their biosynthesis: A review. *Plant Physiol. Biochem.* **2024**, *215*, 108960. [CrossRef]
9. Yan, Y.F.; Li, L.; Zheng, M.Y.; Duan, B.B.; Zhang, J.J.; Li, Y.S.; Liu, W.; Liu, X. Dynamic changes in proanthocyanidin composition, biosynthesis, and histochemistry in spine grape (*Vitis davidii* Foëx) tissues during berry development. *J. Sci. Food Agr.* **2024**, *105*, 2697–2711. [CrossRef]
10. Goufo, P.; Singh, R.K.; Cortez, I. A reference list of phenolic compounds (including stilbenes) in grapevine (*Vitis vinifera* L.) roots, woods, canes, stems, and leaves. *Antioxidants* **2020**, *9*, 398. [CrossRef]
11. Hanzouli, F.; Daldoul, S.; Zemni, H.; Boubakri, H.; Vincenzi, S.; Mliki, A.; Gargouri, M. Stilbene production as part of drought adaptation mechanisms in cultivated grapevine (*Vitis vinifera* L.) roots modulates antioxidant status. *Plant Biol.* **2025**, *27*, 102–115. [CrossRef]
12. Hanzouli, F.; Zemni, H.; Gargouri, M.; Boubakri, H.; Mliki, A.; Vincenzi, S.; Daldoul, S. Evidence of an active role of resveratrol derivatives in the tolerance of wild grapevines (*Vitis vinifera* ssp. *sylvestris*) to salinity. *J. Plant Res.* **2024**, *137*, 265–277. [CrossRef]
13. Fu, M.; Jahan, M.S.; Tang, K.; Jiang, S.Z.; Guo, J.X.; Luo, S.W.; Luo, W.L.; Li, G.H. Comparative analysis of the medicinal and nutritional components of different varieties of *Pueraria thomsonii* and *Pueraria lobate*. *Front. Plant Sci.* **2023**, *14*, 1115782. [CrossRef] [PubMed]
14. Tian, X.; Lv, H.; Xiang, G.; Peng, J.; Li, G.F.; He, Y.; Zhang, F.; Mou, C. Influence of geographic origin and tissue type on the medicinal chemical compounds of *Semiliquidambar cathayensis*. *PeerJ* **2023**, *11*, e15484. [CrossRef] [PubMed]
15. Downey, M.O.; Harvey, J.S.; Robinson, S.P. Synthesis of flavonols and expression of flavonol synthase genes in the developing grape berries of Shiraz and Chardonnay (*Vitis vinifera* L.). *Aust. J. Grape Wine Res.* **2003**, *9*, 110–121. [CrossRef]
16. Yang, Z.Y.; Yin, M.Z.; Cheng, M.G.; Chu, S.S.; Zha, L.P.; Zhao, Y.J.; Peng, H.S. Identification and Functional Characterization of Three Phenylalanine Ammonia-Lyase Genes from *Fallopia multiflora* (Thunb.) Harald. *Russ. J. Bioorg. Chem.* **2023**, *49*, 655–663. [CrossRef]
17. Zeng, Y.; Tian, G.S.; Liu, X.; Chen, L.; Zhu, J.N.; He, F.Y.; Li, K.; Yu, H.; Tang, M.; Yang, Z.T. Integrated metabolomic and transcriptomic analysis of polysaccharides and flavonoids in different tissues of *Houttuynia cordata*. *Sci. Hortic.* **2024**, *338*, 113729. [CrossRef]
18. Ren, R.H.; Chen, H.Z.; Xie, R.; Yuan, H.H.; Xie, S.; Zhang, Z.W. Manganese sulfate application promotes berry flavonoid accumulation in *Vitis vinifera* cv. 'Cabernet Sauvignon' by regulating flavonoid metabolome and transcriptome profiles. *J. Sci. Food Agric.* **2024**, *104*, 1092–1106. [CrossRef]
19. Zhu, T.; He, J.; Li, J.; Liu, C.X.; Min, X.Y.; Hu, X.Y.; Liu, X. Integrative analyses of metabolome and transcriptome reveal regulatory network of puerarin biosynthesis in *Pueraria montana* var. *lobate*. *Molecules* **2024**, *29*, 5556. [CrossRef]
20. Xu, Y.; Huang, D.M.; Ma, F.N.; Yang, L.; Wu, B.; Xing, W.T.; Sun, P.G.; Chen, D.; Xu, B.Q.; Song, S. Identification of key genes involved in flavonoid and terpenoid biosynthesis and the pathway of triterpenoid biosynthesis in *Passiflora edulis*. *J. Integr. Agric.* **2023**, *22*, 1412–1423. [CrossRef]
21. Li, X.; Cao, M.; Ma, W.; Jia, C.H.; Li, J.H.; Zhang, M.X.; Liu, C.C.; Cao, Z.Z.; Faruque, M.O.; Hu, X.B. Annotation of genes involved in high level of dihydromyricetin production in vine tea (*Ampelopsis grossedentata*) by transcriptome analysis. *BMC Plant Biol.* **2020**, *20*, 131. [CrossRef]
22. Wan, L.Y.; Pan, L.M.; Song, L.S.; Fu, J.N.; Huang, Q.L.; Ji, X.W.; Wei, S.G.; Zhang, Z.J. Transcriptional analysis reveals formation of axillary solitary hook in vine plant *Uncaria rhynchophylla*. *Plant Biotechnol. Rep.* **2023**, *17*, 701–713. [CrossRef]
23. Zhao, X.M.; Ge, W.W.; Miao, Z. Integrative metabolomic and transcriptomic analyses reveals the accumulation patterns of key metabolites associated with flavonoids and terpenoids of *Gynostemma pentaphyllum* (Thunb.) Makino. *Sci. Rep.* **2024**, *14*, 8644. [CrossRef]
24. Noronha, H.; Silva, A.; Garcia, V.; Billet, K.; Dias, A.C.P.; Lanoue, A.; Gallusci, P.; Gerós, H. Grapevine woody tissues accumulate stilbenoids following bud burst. *Planta* **2023**, *258*, 118. [CrossRef] [PubMed]
25. Deng, B.; Huang, Z.; Ge, F.; Liu, D.Q.; Lu, R.J.; Chen, C.Y. An AP2/ERF family transcription factor PnERF1 raised the biosynthesis of saponins in *Panax notoginseng*. *J. Plant Growth Regul.* **2017**, *36*, 691–701. [CrossRef]
26. Zhao, B.; Shao, Z.Y.; Wang, L.K.; Zhang, F.; Chakravarty, D.; Zong, W.; Dong, J.; Song, L.; Qiao, H. MYB44-ENAP1/2 restricts HDT4 to regulate drought tolerance in *Arabidopsis*. *PLoS Genet.* **2022**, *18*, e1010473. [CrossRef]
27. Duan, B.L.; Xie, X.F.; Jiang, Y.H.; Zhu, N.; Zheng, H.L.; Liu, Y.X.; Hua, X.J.; Zhao, Y.Y.; Sun, Y.Q. GhMYB44 enhances stomatal closure to confer drought stress tolerance in cotton and *Arabidopsis*. *Plant Physiol. Biochem.* **2023**, *198*, 107692. [CrossRef]

28. Qin, S.S.; Wei, K.H.; Cui, Z.H.; Liang, Y.; Li, M.; Gu, L.; Yang, C.; Zhou, X.; Li, L.; Xu, W.; et al. Comparative Genomics of *Spatholobus suberectus* and Insight Into Flavonoid Biosynthesis. *Front. Plant Sci.* **2020**, *11*, 528108. [CrossRef] [PubMed]
29. Qin, S.S.; Wei, F.; Liang, Y.; Tang, D.F.; Lin, Q.; Miao, J.H.; Wei, K.H. Genome-wide analysis of the R2R3-MYB gene family in *Spatholobus suberectus* and identification of its function in flavonoid biosynthesis. *Front. Plant Sci.* **2023**, *14*, 1219019. [CrossRef]
30. Qin, S.S.; Wei, G.L.; Lin, Q.; Tang, D.F.; Li, C.; Tan, Z.E.; Yao, L.X.; Huang, L.R.; Wei, F.; Liang, Y. Analysis of the *Spatholobus suberectus* full-length transcriptome identified an R2R3-MYB transcription factor-encoding gene *SsMYB158* that regulates flavonoid biosynthesis. *Plant Physiol. Biochem.* **2024**, *214*, 108929. [CrossRef]
31. Pan, Y.H.; Luo, X.M.; Gong, P.Y. *Spatholobi caulis*: A systematic review of its traditional uses, chemical constituents, biological activities and clinical applications. *J. Ethnopharmacol.* **2023**, *317*, 116854. [CrossRef]
32. Cai, J.H.; Aharoni, A. Amino acids and their derivatives mediating defense priming and growth tradeoff. *Curr. Opin. Plant Biol.* **2022**, *69*, 102288. [CrossRef]
33. Oliva, M.; Hatan, E.; Kumar, V.; Galsurker, O.; Nisim-Levi, A.; Ovadia, R.; Galili, G.; Lewinsohn, E.; Elad, Y.; Alkan, N.; et al. Increased phenylalanine levels in plant leaves reduces susceptibility to *Botrytis cinerea*. *Plant Sci.* **2020**, *290*, 110289. [CrossRef]
34. Song, Y.T.; Zhang, G.Y.; Chen, N.; Zhang, J.G.; He, C.Y. Metabolomic and transcriptomic analyses provide insights into the flavonoid biosynthesis in sea buckthorn (*Hippophae rhamnoides* L.). *LWT-Food Sci. Technol.* **2023**, *187*, 115276. [CrossRef]
35. Cheng, J.H.; Xiang, J.; Wei, L.Z.; Zheng, T.; Wu, J. Metabolomic profiling and assessment of phenolic compounds derived from *Vitis davidii* Foex cane and stem extracts. *Int. J. Mol. Sci.* **2022**, *23*, 14873. [CrossRef] [PubMed]
36. Ghafouri, M.; Razavi, F.; Arghavani, M.; Gheshlaghi, E.A. Delaying postharvest senescence and improving antioxidant capacity of kiwifruits cv. Hayward by preharvest selenium application. *J. Food Process. Preserv.* **2022**, *46*, e17185. [CrossRef]
37. Gomez, A.A.; Mercado, M.I.; Belizán, M.M.E.; Ponessa, G.; Vattuone, M.A.; Sampietro, D.A. In situ histochemical localization of alkaloids in leaves and pods of *Prosopis ruscifolia*. *Flora* **2019**, *256*, 1–6. [CrossRef]
38. Wei, K.Q.; Guo, T.T. The changes of tolerance, accumulation and oxidative stress response to cadmium in tobacco caused by introducing *Datura stramonium* L. genes. *Agronomy* **2023**, *13*, 882. [CrossRef]
39. Yonekura-sakakibara, K.; Higashi, Y.; Nakabayashi, R. The origin and evolution of plant flavonoid metabolism. *Front. Plant Sci.* **2019**, *10*, 943. [CrossRef]
40. Wang, Q.; Zhu, J.; Li, B.; Li, S.S.; Yang, Y.; Wang, Q.Y.; Xu, W.Z.; Wang, L.S. Functional identification of anthocyanin glucosyltransferase genes: A Ps3GT catalyzes pelargonidin to pelargonidin 3-O-glucoside painting the vivid red flower color of *Paeonia*. *Planta* **2023**, *257*, 65. [CrossRef]
41. Zan, W.X.; Wu, Q.K.; Dou, S.H.; Wang, Y.T.; Zhu, Z.Q.; Xing, S.T.; Yu, Y.Y. Analysis of flower color diversity revealed the co-regulation of cyanidin and peonidin in the red petals coloration of *Rosa rugosa*. *Plant Physiol. Biochem.* **2024**, *216*, 109126. [CrossRef] [PubMed]
42. Ai, Y.; Zheng, Q.D.; Wang, M.J.; Xiong, L.W.; Li, P.; Guo, L.T.; Wang, M.Y.; Peng, D.H.; Lan, S.R.; Liu, Z.J. Molecular mechanism of different flower color formation of *Cymbidium ensifolium*. *Plant Mol. Biol.* **2023**, *113*, 193–204. [CrossRef]
43. Song, J.X.; Kong, H.M.; Yang, J.; Jing, J.X.; Li, S.Y.; Ma, N.; Yang, R.C.; Cao, Y.M.; Wang, Y.F.; Hu, T.M.; et al. Genome assembly and multi-omic analyses reveal the mechanisms underlying flower color formation in *Torenia fournieri*. *Plant Genome* **2024**, *17*, e20439. [CrossRef]
44. Qiu, L.K.; Zheng, T.C.; Liu, W.C.; Zhuo, X.K.; Li, P.; Wang, J.; Cheng, T.R.; Zhang, Q.X. Integration of transcriptome and metabolome reveals the formation mechanism of red stem in *Prunus mume*. *Front. Plant Sci.* **2022**, *13*, 884883. [CrossRef]
45. Wang, Y.X.; Wang, Z.; Du, H.S.; Chen, B.; Wang, G.Y.; Wang, Q.; Geng, S.S.; Zhang, X.F. Fine mapping of the flavonoid 3′,5′-hydroxylase gene controlling anthocyanin biosynthesis in pepper anthers and stems. *Front. Plant Sci.* **2023**, *14*, 1232755. [CrossRef]
46. Zhang, H.L.; Li, G.Q.; Jiang, M.; Zhao, C.L.; Zhao, P.Y.; Wang, C.; Wen, G.S.; Zhou, F.; Dongchen, W.H.; Xu, S.Z.; et al. Longitudinal expression profiles of flavonoid synthesis-related genes and their correlations with contents of flavonoids including anthocyanins in purplish-green aerial stems of *Panax notoginseng*. *Acta Physiol. Plant.* **2023**, *45*, 3. [CrossRef]
47. Wang, J.Q.; Li, L.; Wang, Z.H.; Feng, A.R.; Li, H.L.; Qaseem, M.F.; Liu, L.T.; Deng, X.M.; Wu, A.M. Integrative analysis of the metabolome and transcriptome reveals the molecular regulatory mechanism of isoflavonoid biosynthesis in *Ormosia henryi* Prain. *Int. J. Biol. Macromol.* **2023**, *246*, 125601. [CrossRef] [PubMed]
48. Guo, D.D.; Zhu, Z.Y.; Wang, Z.; Feng, F.; Cao, Q.; Xia, Z.W.; Jia, X.L.; Lv, D.Y.; Han, T.; Chen, X.F. Multi-omics landscape to decrypt the distinct flavonoid biosynthesis of *Scutellaria baicalensis* across multiple tissues. *Hortic. Res.* **2024**, *11*, uhad258. [CrossRef]
49. Li, M.; Guo, L.; Wang, Y.; Li, Y.Z.; Jiang, X.L.; Liu, Y.J.; Xie, D.Y.; Gao, L.P.; Xia, T. Molecular and biochemical characterization of two 4-coumarate: CoA ligase genes in tea plant (*Camellia sinensis*). *Plant Mol. Biol.* **2022**, *109*, 579–593. [CrossRef] [PubMed]
50. Liu, X.X.; Ma, H.T.; Liu, X.L.; Wang, X.; Chen, Z.J.; Yang, J.; Luo, W.R.; Li, Q.; Yang, F.D.; Li, F. Transcriptomic and metabolomic analyses provide insights into the flavonoid biosynthesis in Dangshen. *Phytochem. Anal.* **2025**, *36*, 1063–1078. [CrossRef]

51. Cao, T.X.; Wang, S.L.; Ali, A.; Shan, N.; Sun, J.Y.; Chen, X.; Wang, P.T.; Zhu, Q.L.; Xiao, Y.; Luo, S.; et al. Transcriptome and metabolome analysis reveals the potential mechanism of tuber dynamic development in yam (*Dioscorea polystachya* Turcz.). *LWT-Food. Sci. Technol.* **2023**, *181*, 114764. [CrossRef]
52. Lu, Y.; Song, Y.Y.; Zhu, J.; Xu, X.G.; Pang, B.; Jin, H.; Jiang, C.M.; Liu, Y.L.; Shi, J.L. Potential application of *CHS* and *4CL* genes from grape endophytic fungus in production of naringenin and resveratrol and the improvement of polyphenol profiles and flavour of wine. *Food Chem.* **2021**, *347*, 128972. [CrossRef]
53. Xu, C.; Xue, X.; Li, Z.; Chen, M.G.; Yang, Y.T.; Wang, S.Y.; Shang, M.R.; Qiu, L.; Zhao, X.Y.; Hu, W.X. The PpMYB75-PpDFR module reveals the difference between 'SR' and its bud variant 'RMHC' in peach red flesh. *J. Plant Res.* **2024**, *137*, 241–254. [CrossRef]
54. Devi, A.; Masand, M.; Sharma, B.; Majeed, A.; Sharma, R.K. Integrated transcriptome and metabolome analysis decrypting molecular insights of specialized metabolism in *Valeriana jatamansi* Jones. *Ind. Crops Prod.* **2024**, *214*, 118504. [CrossRef]
55. Xia, Y.Y.; Su, Q.; Li, X.; Yan, S.; Liu, J.Y.; He, C.F.; Huang, H.J.; Jiang, W.B.; Pang, Y.Z. Two CYP93A enzymes play a dual role in isoflavonoid biosynthesis in *Glycine max* L. *Plant Physiol. Biochem.* **2023**, *203*, 108073. [CrossRef]
56. Han, H.; Dong, L.W.; Zhang, W.W.; Liao, Y.L.; Wang, L.N.; Wang, Q.J.; Ye, J.; Xu, F. *Ginkgo biloba* GbbZIP08 transcription factor is involved in the regulation of flavonoid biosynthesis. *J. Plant Physiol.* **2023**, *287*, 154054. [CrossRef]
57. Kong, W.L.; Zhao, P.; Zhang, Q.; Yang, J.J.; Zhu, Q.F.; Zhang, Y.B.; Deng, X.M.; Chen, X.; Lin, J.K.; Zhang, X.T. Chromatin accessibility mediated transcriptome changes contribute to flavor substance alterations and jasmonic acid hyperaccumulation during oolong tea withering process. *Plant J.* **2024**, *117*, 679–693. [CrossRef]
58. Qiao, F.; Zhang, K.M.; Zhou, L.Y.; Qiu, Q.S.; Chen, Z.N.; Lu, Y.H.; Wang, L.H.; Geng, G.G.; Xie, H.C. Analysis of flavonoid metabolism during fruit development of *Lycium chinense*. *J. Plant Physiol.* **2022**, *279*, 153856. [CrossRef]
59. Shan, T.Y.; Xu, J.Y.; Zhong, X.X.; Zhang, J.J.; He, B.; Tao, Y.J.; Wu, J.W. Full-length transcriptome sequencing provides new insights into the complexity of flavonoid biosynthesis in *Glechoma longituba*. *Physiol. Plant.* **2023**, *175*, e14104. [CrossRef]
60. Jiang, Z.F.; Liu, D.D.; Wang, T.Q.; Liang, X.L.; Cui, Y.H.; Liu, Z.H.; Li, W.B. Concentration difference of auxin involved in stem development in soybean. *J. Integr. Agric.* **2020**, *19*, 953–964. [CrossRef]
61. Xing, M.Y.; Cao, Y.L.; Ren, C.H.; Liu, Y.L.; Li, J.J.; Grierson, D.; Martin, C.; Sun, C.D.; Chen, K.S.; Xu, C.J.; et al. Elucidation of myricetin biosynthesis in *Morella rubra* of the Myricaceae. *Plant J.* **2021**, *108*, 411–425. [CrossRef]
62. Pasternak, T.; Yaroshko, O. Molecular biology needs a map: Spatial in situ approaches in plant science. *Plant Biol.* **2026**, *28*, 323–327. [CrossRef]
63. Muhammad, N.; Luo, Z.; Zhao, X.; Yang, M.; Liu, Z.G.; Liu, M.J. Transcriptome-wide expression analysis of MYB gene family leads to functional characterization of flavonoid biosynthesis in fruit coloration of *Ziziphus Mill*. *Front. Plant Sci.* **2023**, *14*, 1171288. [CrossRef]
64. Wang, F.; Yang, F.; Zhu, D.; Saniboere, B.; Zhou, B.; Peng, D. MYB44 plays key roles in regulating plant responses to abiotic and biotic stress, metabolism, and development. *J. Plant Biochem. Biotechnol.* **2024**, *33*, 462–473. [CrossRef]
65. Song, Y.; Ma, B.; Guo, Q.X.; Zhou, L.X.; Lv, C.Y.; Liu, X.M.; Wang, J.L.; Zhou, X.T.; Zhang, C.Y. UV-B induces the expression of flavonoid biosynthetic pathways in blueberry (*Vaccinium corymbosum*) calli. *Front. Plant Sci.* **2022**, *13*, 1079087. [CrossRef] [PubMed]
66. Ma, R.X.; Sun, X.Z.; Yang, C.; Fan, Y.L. Integrated transcriptome and metabolome provide insight into flavonoid variation in goji berries (*Lycium barbarum* L.) from different areas in China. *Plant Physiol. Biochem.* **2023**, *199*, 107722. [CrossRef]
67. Huang, H.; Yao, Q.Y.; Xia, E.H.; Gao, L.Z. Metabolomics and transcriptomics analyses reveal nitrogen influences on the accumulation of flavonoids and amino acids in young shoots of tea plant (*Camellia sinensis* L.) associated with tea flavor. *J. Agric. Food Chem.* **2018**, *66*, 9828−9838. [CrossRef]
68. Wang, F.; Ge, S.F.; Xu, X.X.; Xing, Y.; Du, X.; Zhang, X.; Lv, M.X.; Liu, J.Q.; Zhu, Z.L.; Jiang, Y.M. Multiomics Analysis Reveals New Insights into the Apple Fruit Quality Decline under High Nitrogen Conditions. *J. Agric. Food Chem.* **2021**, *69*, 5559−5572. [CrossRef] [PubMed]
69. Zhao, C.N.; Liu, X.J.; Gong, Q.; Cao, J.P.; Shen, W.X.; Yin, X.R.; Grierson, D.; Zhang, B.; Xu, C.J.; Li, X.; et al. Three AP2/ERF family members modulate flavonoid synthesis by regulating type IV chalcone isomerase in citrus. *Plant Biotechnol. J.* **2021**, *19*, 671–688. [CrossRef]
70. Song, W.L.; Zhang, S.Y.; Li, Q.; Xiang, G.S.; Zhao, Y.; Wei, F.; Zhang, G.H.; Yang, S.C.; Hao, B. Genome-wide profiling of WRKY genes involved in flavonoid biosynthesis in *Erigeron breviscapus*. *Front. Plant Sci.* **2024**, *15*, 1412574. [CrossRef]
71. Wan, H.L.; Liu, Y.H.; Wang, T.T.; Jiang, P.; Wen, W.W.; Nie, J.Y. Combined transcriptomic and metabolomic analyses identifies CsERF003, a citrus ERF transcription factor, as flavonoid activator. *Plant Sci.* **2023**, *334*, 111762. [CrossRef] [PubMed]

Disclaimer/Publisher's Note: The statements, opinions and data contained in all publications are solely those of the individual author(s) and contributor(s) and not of MDPI and/or the editor(s). MDPI and/or the editor(s) disclaim responsibility for any injury to people or property resulting from any ideas, methods, instructions or products referred to in the content.